*Journal of Fluids and Structures* (2001) **15,** 1031–1060
doi:10.1006/jfls.2001.0385, available online at http://www.idealibrary.com on IDEAL®

# FLOW AND DISPERSION IN GROUND VEHICLE WAKES

C. J. Baker

*School of Civil Engineering, University of Birmingham*
*Edgbaston, Birmingham, B15 2TT, U.K.*

(Received 1 November 2000, and in final form 9 February 2001)

This paper considers the flow velocities and the dispersion of pollutants in the wake of a number of different types of ground vehicles. It does this mainly through a collation of the results of a number of experimental, numerical and analytical investigations carried out by the author and his co-workers over the last few years, and a comparison of these results with the work of other investigators. It is shown that the wakes of ground vehicles may be conveniently taken to consist of two regions: a near wake and a far wake. The near wake is characterised by large scale recirculation and longitudinal vortex structures, with unsteady fluctuations caused by a variety of effects, including instability of the separated shear layer and wake pumping. In the far wake there are no discernible flow structures with a steady decay of the velocity field, with the major component of wake unsteadiness being at large scales. The effect of cross-winds is to translate and diffuse the wake, with the balance between the two effects changing depending upon the nature of the surrounding topography. Only a relatively few measurements have been made of dispersion within vehicle wakes, other than in the rather complex case of vehicles in street canyons. However, there are a number of analytical solutions of wake dispersion that have, to some extent, been validated by comparison with full-scale experiments. On the basis of these investigations, it is suggested that the lower frequency fluctuations in vehicle wakes may have an effect on the dose of pollutants received by pedestrians at the roadside, and more work is suggested to quantify this further.


## 1. INTRODUCTION

### 1.1. Background

It is now widely acknowledged that vehicle emissions have a significant and damaging effect on human health. These pollutants are both gaseous (carbon monoxide, oxides of nitrogen, hydrocarbons, etc.) and particulate (carbon, car and tyre components, road dust, etc). These pollutants and the legal limits for concentration levels are usefully outlined in IHT (1999) and in many other sources. From the viewpoint of an engineer, it is necessary to be able to calculate the dispersion of these pollutants away from the roadway, and a number of methods exist for doing this. Amongst the models in most common use are CALINE (Benson *et al.* 1979), HIWAY (Rao & Keenan 1980), ROADWAY (Eskridge & Hunt 1979; Eskridge *et al.* 1979), CPBM (Yamartino & Wiegand 1986) and OPSM (Berkowicz *et al.* 1994). Now it has been acknowledged by a number of authors that the wakes of ground vehicles have a significant effect on the dispersion of vehicle pollutants. However, most pollutant dispersion models represent the source of traffic pollutants as simple line sources of pollutant (which is obviously a major simplification of the actual situation of a large number of moving point sources), and vehicle wakes are usually either ignored completely or represented by a simple enhancement of turbulence levels (and thus mixing) close to the

0889–9746/01/071031 + 30 $35.00/0 

line source. [Note that the major exception to this is the ROADWAY model based on the work of Eskridge & Hunt (1979) which will be discussed below]. Vehicle wakes have been much studied in the past, largely by those interested in the aerodynamic behaviour of ground vehicles, and in particular the effect of wake structures on vehicle drag; see, for example, the work of Maull (1978) and Ahmed (1981). Little attention has been paid to those properties of wakes which are connected with the dispersion of pollutants. In short, there is little interaction between the studies of the vehicle aerodynamicist, and pollution dispersion modellers. An example of this at a trivial level is that even the coordinate systems used by the two groups are often different, with the $z$-axis being in the horizontal plane perpendicular to the vehicle direction of travel for the former, and vertically upward for the latter. This lack of dialogue is unfortunate, since the insights of vehicle aerodynamics investigations are potentially of significant use to the pollution dispersion modelling community in the specification of boundary conditions and source strengths, etc. This paper attempts to fill this gap, by considering the development of the wakes of ground vehicle from close to the vehicle to many vehicle heights downstream, and by considering the dispersion of pollutants within these wakes. It does so primarily by a correlation of the results of a number of investigations carried out by the author and his co-workers over recent years, together with the results of other investigators.

Section 1.2 presents brief details of the various investigations that will be used. These include wind-tunnel and numerical investigations of the wakes of cars, lorries and high speed trains, and experimental, numerical and full-scale determinations of the nature of pollutant dispersion within wakes. Section 2 then describes vehicle wake flow patterns. Two basic flow regions are distinguished: the near wake and the far wake, and the different nature of the flow in the two regions is considered. The effects of cross-winds and urban topography (street canyons) on vehicle wake flows are also discussed. Section 3 considers the nature of pollution dispersion in the near and far wakes, and again considers the effects of cross-winds and urban topography. A discussion of the full-scale context is also presented, which involves a discussion of the appropriate time scales involved in pollutant concentration fluctuations. Finally, in Section 4 some concluding remarks are made and future research needs to be identified.

## 1.2. The Investigations

Over the last ten years, the author has supervised a number of investigations of different types that are of relevance to this paper. These are briefly described below in four categories: model-scale experiments to measure vehicle wake parameters, model-scale experiments to measure pollutant dispersion, theoretical and computational studies, and full-scale measurements. These are presented in turn below.

### *1.2.1. Model scale measurements of wake parameters*

(a) *Measurements behind cars.* Richards *et al.* (2000a, b) present preliminary results of flow measurements in the wake of a 1/3 scale model of the MIRA reference car in fastback formation. The results that have been obtained included detailed wake traverses in the near-wake region using hot-wire anemometers. Results are presented for the three velocity components and for turbulent kinetic energy. Further unpublished work from this investigation will be presented in this paper, in particular details of the unsteady nature of the wake flow.

(b) *Measurements behind lorries.* Coleman & Baker (1994) investigated the flow field around a 1/50 scale model of an articulated lorry, mainly at large yaw angles, as they were

principally interested in the overturning of such vehicles in cross-winds. Baker *et al.* (2000) describe experiments carried out with a 1/25 scale model of the same vehicle. These experiments were carried out using a moving model rig, which could fire the vehicle at high speeds along a 200 m test track. The vehicle slipstreams and wakes were measured using rakes of hot-film anemometers. Thus time histories of slipstream and wake velocities were obtained. To enable these to be analysed it was necessary to form ensemble averages of a large number of runs of the rig. In this paper, the work of Baker *et al.* (2000) will be taken further, particularly in terms of an investigation of the unsteady nature of the velocity time histories in the wake region.

(c) *Measurements behind trains.* Baker *et al.* (2001) present data similar to the lorry experiments described above for the flow around a 1/25 scale model of a high-speed passenger train—the DB (German Railways) ICE.

### *1.2.2. Model-scale measurements of dispersion*

(a) *Dispersion behind cars.* Richards *et al.* (2000a, b) describe wind-tunnel measurements of gaseous dispersion in the wake of the 1/3 scale MIRA reference car. The pollutant (propane) was injected into the flow at the exhaust position, and fast response flame ionisation detectors were used to obtain the mean and fluctuating values of wake concentrations.

(b) *Dispersion behind lorries.* Baker & Hargreaves (2001) describe experiments using the 1/50 scale lorry model used by Coleman & Baker (1994). The model was placed on a moving model rig and was propelled across a wind tunnel in which an atmospheric boundary layer had been simulated. Propane was injected into the flow from the lorry exhaust position as the lorry was fired across the tunnel, and concentrations downstream of the model were measured using flame ionisation detectors. Experiments were carried out both with an open country wind simulation and with a street canyon wind simulation.

(c) Pearce & Baker (1997, 1999) carried out a thorough wind-tunnel investigation of pollutant dispersion within an urban area (the city of Leicester in the English midlands). A line source of pollutant along the centre of a major highway was used. However, to simulate the effect of vehicle movement on pollutant dispersion, the wind-tunnel model of the city area was placed above the moving model rig also used by Hargreaves & Baker (2000), and a "train" of car-like blocks fired across the tunnel above the line source. These tests thus illustrated the effect of moving vehicles on pre-existing clouds of pollutant.

### *1.2.3. Theoretical and numerical approaches*

(a) *Flow and dispersion behind cars.* Richards *et al.* (2000a, b) report on CFD calculations of the flow field and dispersion around their model car, using a full simulation of the vehicle within the wind tunnel.

(b) *General wake studies.* Baker (1996) presents a method for calculating the pollutant concentrations in vehicle wakes, based upon a Gaussian puff model of pollutant transport. This model allows some interesting results to be obtained on the nature of pollutant concentrations from vehicles in a cross-wind and the effect of such parameters as traffic density and emission rates. Hargreaves & Baker (1997) develop this method further to allow pollutant concentrations within street canyons to be determined. Hider (1998) describes a development of the analysis of Eskridge & Hunt (1979) for the calculation of vehicle wake flow fields, and goes on to consider the movement of particulate pollutants within vehicle wakes.

*1.2.4. Full-scale measurements*

(a) *Vehicle pressure fields.* Quinn *et al.* (2000) describe an investigation to measure wind- and vehicle-induced loads on temporary road signs at the side of roads. They showed that, for typical road sign positions, the effect of passing vehicles was almost entirely due to the pressure pulse created by the vehicle, rather than by air movement in vehicle wakes. They were able to quantify these pressure pulses, and the loads that were associated with them.

(b) *Full-scale pollutant concentration measurements.* Namdeo *et al.* (1999) describe experiments to measure the roadside concentrations of particulate pollutants. They utilised optical aerosol spectrometers that were able to make measurements of pollutant concentrations over a number of size ranges, with averaging times of between 6 s and 1 h. Concurrent measurements were also made of traffic flow conditions.

In what follows, experimental and theoretical results from a wide variety of different investigations will be presented. To enable comparisons to be made between them, the results and their position of measurement will be expressed as far as possible in a dimensionless form. Essentially the main parameters used in the nondimensionalisation will be the vehicle height $h$ and the vehicle speed (or wind-tunnel speed) $u$. The coordinate system that is used has an origin at ground level at the rear of the vehicle, with the dimensionless distances from that point, in the longitudinal, lateral and vertical directions, given by $X$, $Y$ and $Z$, respectively. The dimensionless velocities in these directions are $U$, $V$ and $W$. The lower case variable $y$ will be used to denote distance from the side of the vehicle. For the various moving model experiments, it is appropriate to define a dimensionless time $T$ as $tu/h$, where $t$ is the time since the rear of the vehicle passed the measurement point. Thus $T$ and $X$ are effectively equivalent. Finally, a dimensionless frequency $F$ of fluctuations is defined as $fh/u$.

Most of the data that will be presented in what follows have not been previously published, or they have been significantly reworked for the current paper. Where this is not the case, it is clearly indicated in the text and in the figure captions.

## 2. VEHICLE WAKE FLOW PATTERNS

### 2.1. Wake Regions

Figure 1 shows ensemble average time histories of the dimensionless longitudinal velocity behind 1/25 scale models of a lorry and a high speed train. These were measured using a rake of stationary hot-film anemometers placed horizontally close to the height of the vehicle centre line, whilst the models were fired along a high-speed test track (Baker *et al.* 2000, 2001). Note that this method of measurement means that the results that are presented are for the velocity normal to the hot film, which consists of both a longitudinal and a lateral component. For most of the results presented here, however, cross-wire measurements suggested that the lateral component is small and the measurements effectively indicate the longitudinal velocity with only small error. For the train results, the ensemble averages were formed from around 20 separate runs, whilst for the lorry case they were formed from around 10 runs. Eight hot films were used, but for clarity only the results of three are shown. It can be seen that there is considerable variation in the velocity time histories for around 10–20 vehicle heights downstream, but after that the velocities decay in a regular manner. The details of these figures will be discussed below.

Figure 2 shows velocity profiles for the cases of Figure 1, at a number of different nondimensional times, i.e. these are effectively slices across Figure 1. It can be seen that there is a general decay in the velocity profiles as $T$ increases.

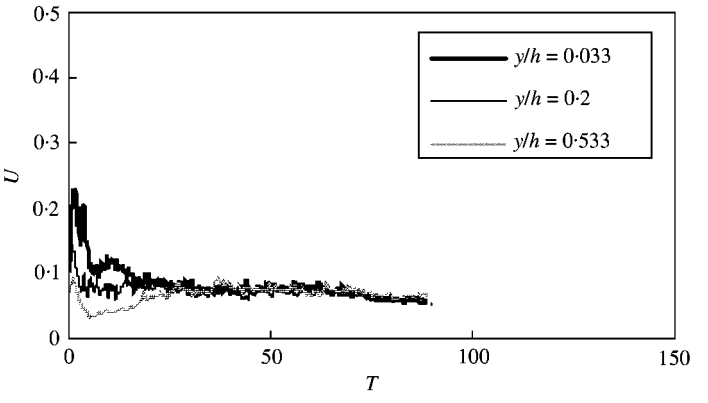


(a) Lorry results

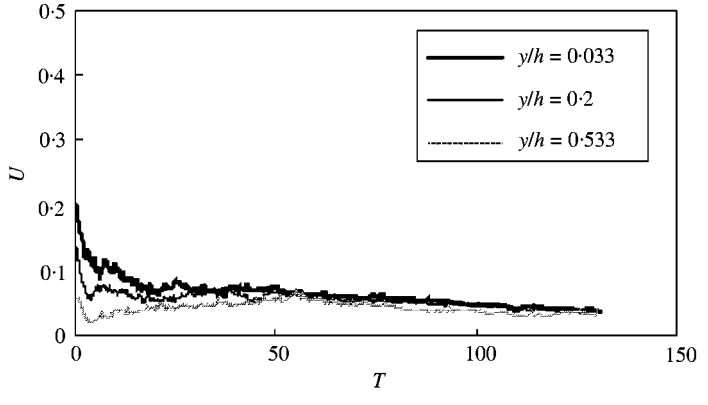


(b) Train results

Figure 1. Ensemble averaged velocity time histories for lorry and train models from moving model experiments. (Velocities measured with hot films mounted at model mid height in horizontal line normal to the vehicle side, nominal model speed of 30 m/s. See Baker *et al.* (2000, 2001) for experimental details.)

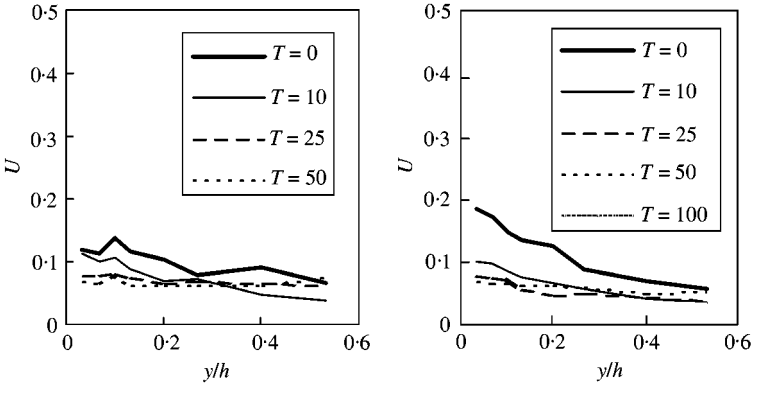


(a) Lorry results (b) Train results

Figure 2. Ensemble averaged wake velocity profiles for lorry and train models from moving model experiments (Velocities measured with hot films mounted at model mid height in horizontal line normal to the vehicle side, nominal model speed of 30 m/s. See Baker *et al.* (2000, 2001) for experimental details.)

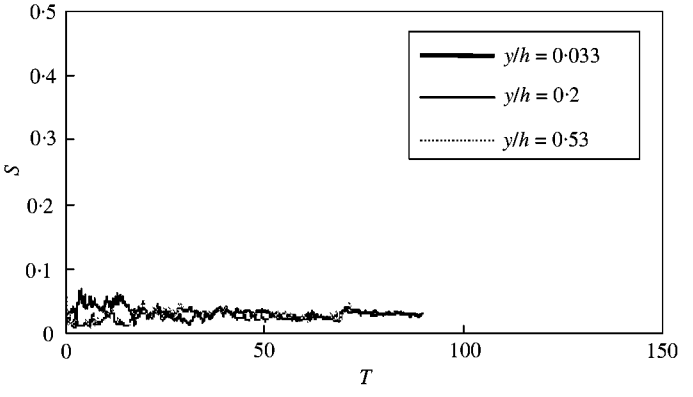


(a) Lorry results

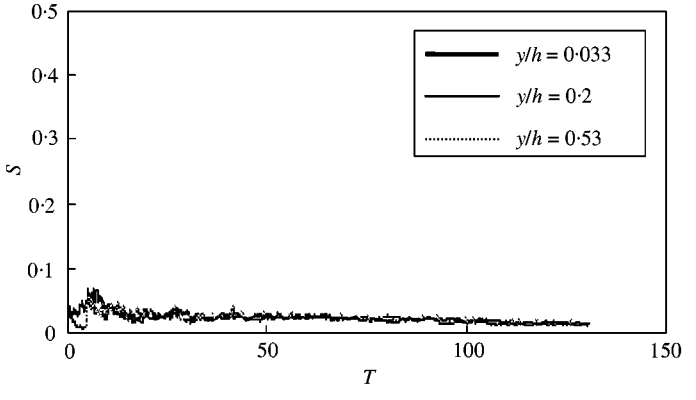


(b) Train results

Figure 3. Standard deviations of ensemble averaged velocities for lorry and train models from moving model experiments. (Velocities measured with hot films mounted at model mid height in horizontal line normal to the vehicle side, nominal model speed of 30 m/s. See Baker *et al.* (2000, 2001) for experimental details.)

Figure 3 shows the nondimensional standard deviations $S$ of the ensemble averages for the results of Figure 1. These can be seen to be substantially close to the vehicle (for $T < 10$), but then gradually decay in line with the average profiles of Figure 1.

Figure 4 shows wavelet spectra downstream of the models. These were obtained using a Morlet wavelet base, and effectively represent instantaneous spectra at different dimensionless times (Torrence & Compo 1998). The analysis has been carried out for individual runs of the models on the moving model rig, and an ensemble average formed of the wavelet spectra. It is normal to plot the wavelet power against a wavelet scale, which, for the Morlet wavelet used, is very close to the inverse of the Fourier frequency. To aid comparison with results that are shown later, the wavelet power $W$ multiplied by dimensionless Fourier frequency $F$ is plotted against $F$. The results are plotted in a linear-log form, so the area between any two frequencies on the graphs is a true representation of the power between these frequencies. Again these results will be described in more detail below. The important thing to note here is that, for low values of $T$, there is a large peak in the spectra at a value of $F$ of about 0·5. It will be argued below that this is associated with the separated shear layers from the vehicle. This peak decays rapidly however, and for the lorry results it has disappeared by approximately $T = 5$, while for the train results by approximately $T = 10$.

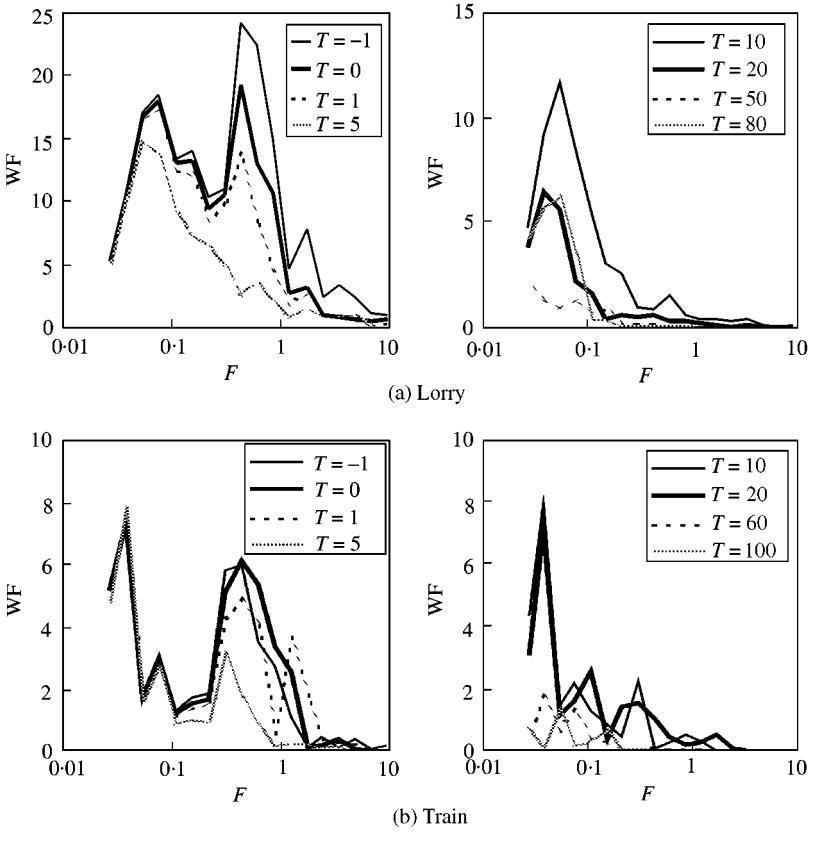


Figure 4. Wavelet spectra of velocity time histories for lorry and train models from moving model experiments. (Velocities measured with hot films mounted at model mid height in horizontal line normal to the vehicle side, nominal model speed of 30 m/s. See Baker *et al.* (2000, 2001) for experimental details.)

Thus, from what has been said, it seems that, for the two vehicles considered, there is a difference in wake structure before and after a dimensionless time of $T = 10$. In the following sections we will describe dimensionless times of less than this as corresponding to the near wake, and times greater than this as corresponding to the far wake. This definition is of course somewhat arbitrary, and is only defined here for two vehicle types, but nonetheless serves as a useful concept.

## 2.2. Near Wake

In aerodynamic terms, cars can be conveniently divided into a number of categories, which are, in the order of decreasing base bluntness: (a) squareback, with a bluff trailing end; (b) notchback, with a distinct horizontal top to the boot behind the passenger compartment; (c) fastback, with a sloping rear surface. Many of the idealised car shapes used in wind-tunnel experiments can be regarded as extreme examples of the fastback configuration.

It is a well-appreciated fact by a number of authors that, in general, the near wake of a car consists of two components: a large scale recirculation region immediately behind the vehicle and a system of longitudinal trailing vortices (Hucho 2000). This was first illustrated very convincingly by Ahmed (1981) who studied the flow around a number of car models,

with different rear end geometries and different levels of detail. He showed that in general, the recirculation region decreased in extent as the rear-end slope decreased, i.e., as the vehicle rear became more streamlined. He found that this recirculation consisted of two regions of opposite sense of rotation, one on top of the other, and extended to values of $X$ between 0·4 and 0·7, with the larger values for the squareback vehicles. Duell *et al.* (1999), for a blunt vehicle shape, measured a separation bubble of length $X = 1{\cdot}1$. The strength of the longitudinal trailing vortex system was found to be greatest for those vehicles with the most "streamlined" rear end shapes, i.e. notchbacks and fastbacks. For the blunter sqare-back shapes the vortices ceased to be well defined to $X = 1{\cdot}5$, whilst for the more streamlined shapes they could still be discerned at $X = 3$. Similar trends have been observed by a number of other authors—for example Bearman *et al.* (1983) (who could still discern the longitudinal vortices around an idealised vehicle shape (fastback) at $X = 6{\cdot}5$), Nouzawa *et al.* (1992) for a fastback configuration, and most recently Richards *et al.* (2000a, b), also for a fastback configuration. Some sample results of the latter are shown in Figures 5(a, b), which show the lateral and vertical velocities at $X = 0{\cdot}42$ (which is in this case close to the end of the recirculation region), and the trailing vortex pattern can be clearly identified from the indicated flow directions. The calculated velocities found using a commercial $k$–$\varepsilon$ CFD package (with a nonlinear turbulence model and an upwind differencing solver) are also shown, and the agreement can be seen to be reasonably good. It is of interest to note, however, that the CFD calculation was unable to represent the two-tier structure of the separation region that was measured in the experiments. Figure 5(c) shows the turbulent kinetic energy within the wake from both experiments and from the CFD calculations. It can be seen that the calculations somewhat underpredict the turbulence levels in the wake, but the general distribution is adequately predicted.

Duell & George (1992, 1993, 1999) made measurements in the wake of an idealised vehicle shape with a squareback configuration and were able to distinguish two discrete frequency peaks in the vehicle wake. The lowest peak corresponded to a value of $F$ of 0·069 and was attributed to "wake pumping"—an overall longitudinal oscillation of the separated region. The higher value of $F$ was around 1·15 and was found to be associated with an instability in the separated shear layers. Evidence was presented of vortex pairing that reduced the value of $F$ by factors of 2 at intervals along the near wake (i.e., to values of 0·57, 0·28, 0·14 and the "pumping" frequency of 0·07. Sims-Williams *et al.* (2001) report measurements of the unsteady flow field behind a variety of notchback vehicles at a number of different scales in a number of different wind tunnels. They found weak fluctuations within the near wake at values of $F$ of between 0·3 and 0·6, depending upon which wind tunnel was used as well as wind-tunnel speed. There was no apparent reason for the variation, which they concluded was partly due to the nature of the turbulence in the ambient wind-tunnel flow. No low-frequency peak was observed in these experiments. Bearman (1997) presents the results from a fastback configuration and shows that these longitudinal trailing vortex patterns are inherently unsteady, and that instantaneous PIV results show distributed vorticity across the vehicle wake. Thus these vortices can be defined in a mean sense only (Figure 6). He also reports on hot-wire measurements in the vehicle wake that revealed a peak in the power spectrum at a nondimensional frequency $F$ of about 0·4–0·5. A similar value of 0.42 can be inferred from the results of Nouzawa *et al.* (1992) for a fastback car. The investigation of Richards *et al.* (2000) for a fastback configuration has also included many measurements of power spectra in the vehicle wake. Typical spectra are shown in Figure 7 for various points along the wake, from the end of the recirculation region downstream. Most of the fluctuating energy can be seen at values of $F$ of 0·5 for the measurement position nearest the vehicle, increasing to 1·0 further away from the vehicle.

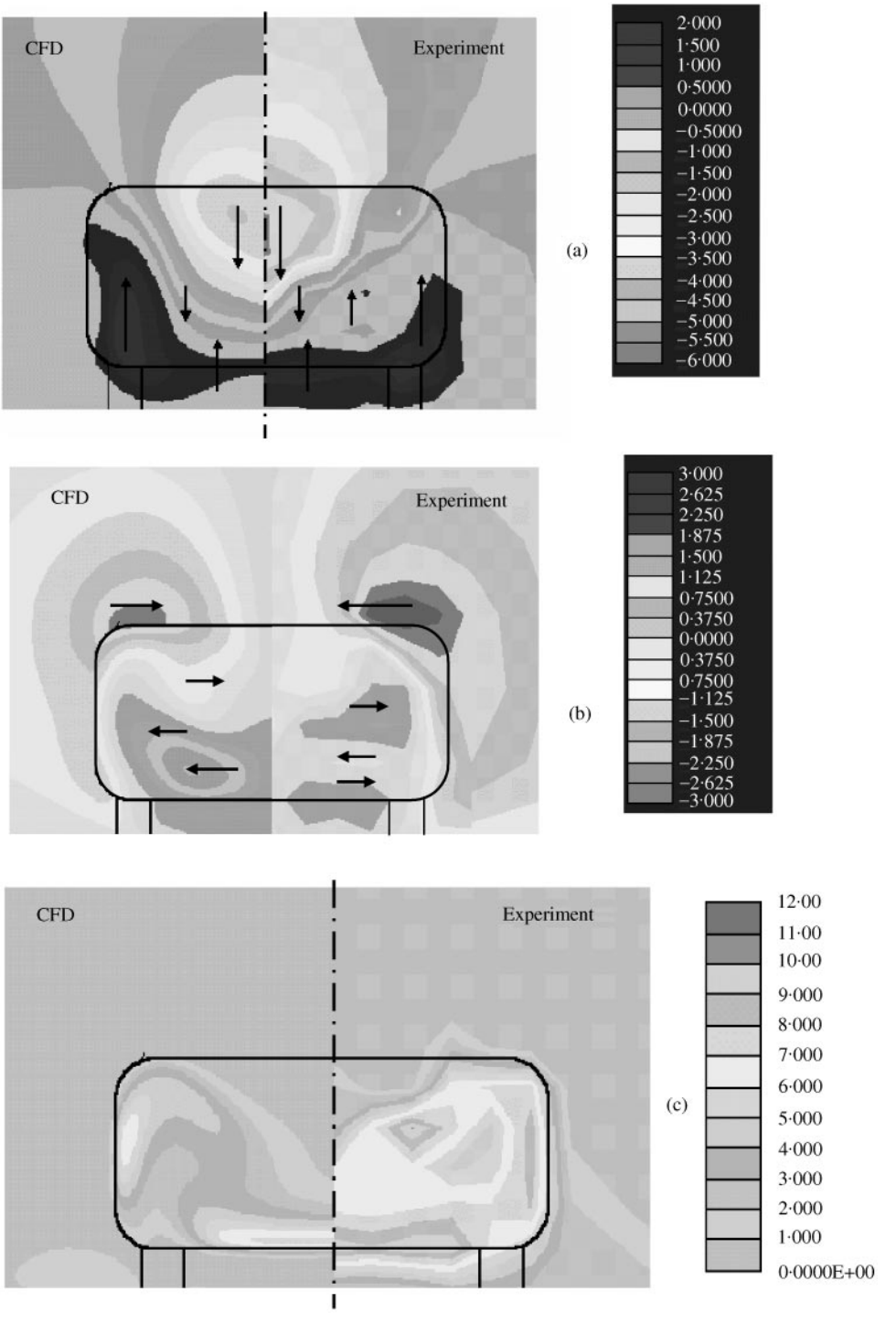


Figure 5. Experimental and CFD measurements of (a) vertical velocity component, (b) lateral velocity component, (c) turbulent kinetic energy for 1/4 scale car model (CFD results on left, experimental results on right; results at $X = 0{\cdot}42$, wind speed $= 13$ m/s. CFD results were obtained with an upwind differencing scheme and a non linear $k$–$\varepsilon$ turbulence model. See Richards *et al.* (2000a, b) for further details.)

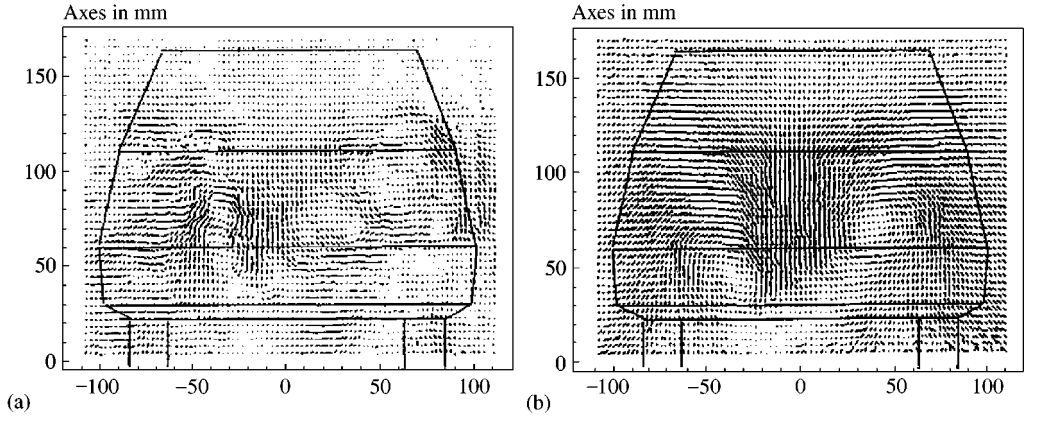


Figure 6. Instantaneous and averaged PIV results in the wake of a car taken from Bearman (1997). Left figure is an individual PIV measurement, right figure is average of 10 measurements.

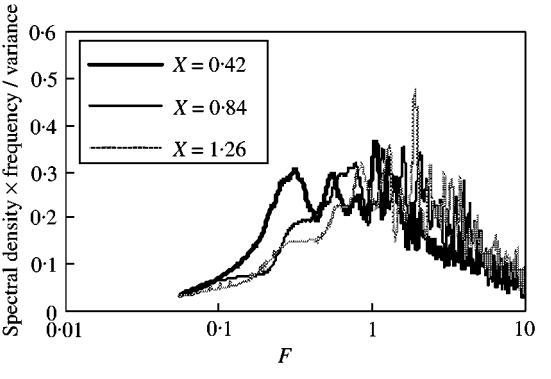


Figure 7. Velocity spectra in the wake of a car. (Measurements are made at $Y = 0{\cdot}21$ and $Z = 0{\cdot}36$, with a wind tunnel speed of 13 m/s; see Richards *et al.* (2000b) for experimental details.)

Now consider the results for the lorry model shown in Figures 1–4. The velocity time histories of Figure 1, the profiles of Figure 2 and the standard deviations of Figure 3 show large rates of change of velocity in the near-wake region, both in the direction of travel, and normal to it. The large values of standard deviation of the ensemble average results show that there is considerable run-to-run variation within this region. Now, the flow field in this region can be expected to consist of separated shear layers from the model surface that surround a large scale flow recirculation immediately behind the vehicle. Further light is shed on the relationship between these mechanisms in the wavelet spectra of Figure 4. The near wake results for the lorry show two peaks in the spectra—one at low frequencies ($F = 0{\cdot}05$–$0{\cdot}1$) and one at higher frequencies ($F = 0{\cdot}5$). The higher frequency peak also appears at a value of dimensionless time $T$ of $-1$ (i.e., before the separation of the wake shear layers), showing that it is associated with some dominant length scale of the turbulence in the vehicle boundary layer. For values of $T$ greater than zero, this peak decays rapidly, and a more detailed examination of the data shows that it cannot be distinguished for $T > 3$. The low frequency peak grows in magnitude as $T$ increases. Whilst one must be somewhat circumspect about the interpretation of peaks in the wavelet spectra at frequencies that correspond to scales that are close to the overall scale of the data used in the

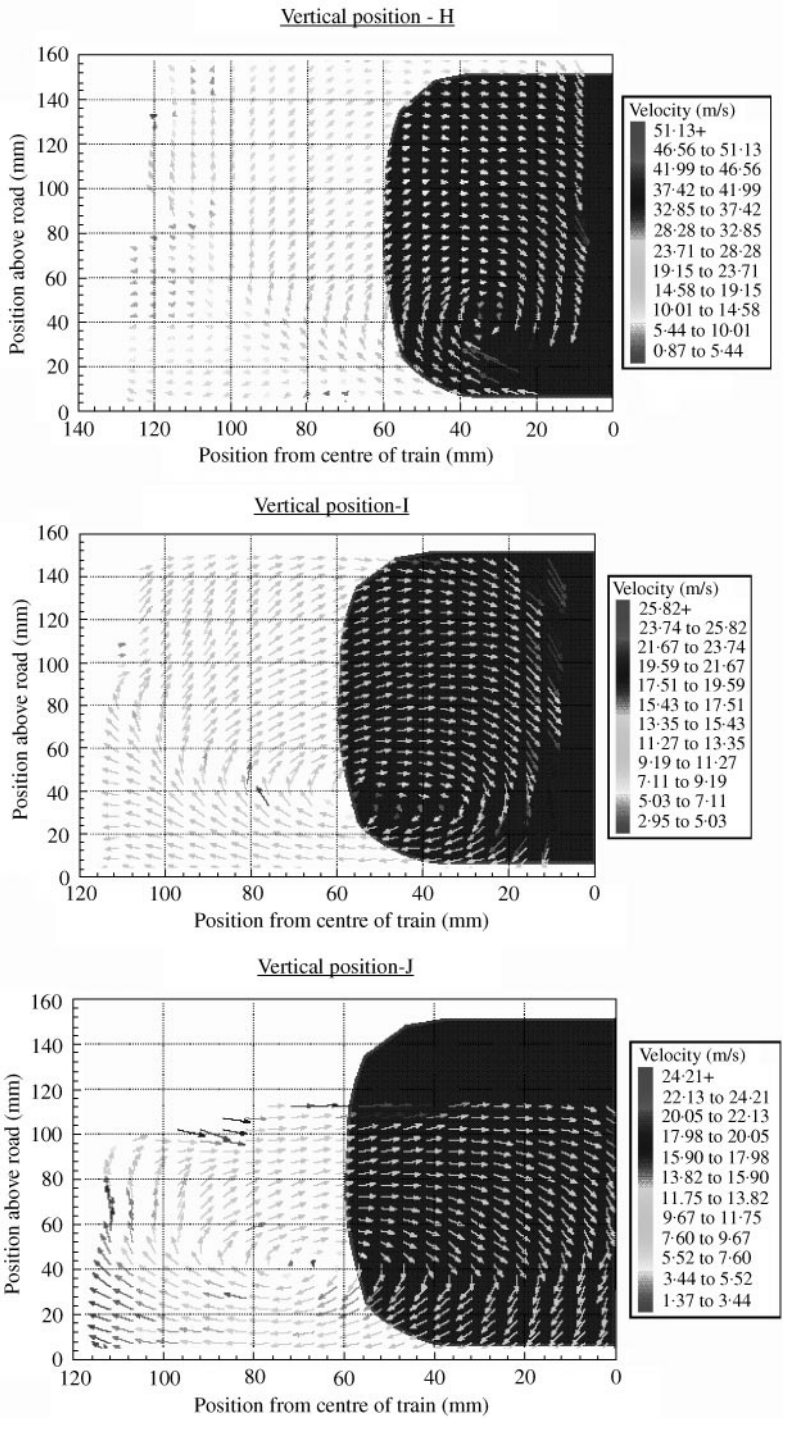


Figure 8. PIV measurements in wake of high speed train taken from Baker *et al.* (2001). (Sections H, I and J are at $X = 0{\cdot}066$, $1{\cdot}03$ and $2{\cdot}00$, respectively, wind-tunnel speed $= 40$ m/s. Results supplied by the Scott Flow Dynamics.)

doi:10.1006/jfls.2001.0385

analysis (a dimensionless time of about 100, and thus a dimensionless frequency of 0.01) it seems likely that this lower frequency peak is due to the unsteadiness of the wake as a whole, i.e., it represents the vehicle-passing effect. These considerations thus suggest that the flow structure in the wake is a complex mix of fluctuations due to shear layer oscillation, and oscillation of the overall wake structure, with the former decaying rapidly with $T$ and the latter becoming more dominant.

Next, consider the train results of Figures 1–4. These results are similar in many ways to the lorry results just discussed, but there are some interesting differences. Firstly, the standard deviations of the ensemble averages are somewhat lower, and the velocity profiles are rather smoother. This may be because more runs were used in the analysis of the data than for the lorry, but they do actually suggest a rather better defined flow than in the lorry case. Secondly, the wavelet spectra show that the peak associated with the unsteadiness in the vehicle boundary layer persists significantly further downstream for the train than for the lorry, and the lower frequency peak is not so large. These low frequency oscillations are at rather lower values of $F$ of around 0·03. Now, in this regard, it is interesting to consider the PIV results obtained as part of the project described in Baker *et al.* (2001) (Figure 8) for a static model in a wind tunnel. These were obtained in the near-wake region at values of $X$ of 0·066, 1·03 and 2·0 and show the existence of a longitudinal trailing vortex pair behind the train that gradually moves away from the train centreline. Similar results have been obtained from CFD calculations by Matschke & Heine (2000) for a similar high speed train (Figure 9). It can thus be conjectured that for the case of a high speed train with a streamlined tail shape, much of the energy in the near wake is associated with the trailing vortex pair at frequencies that are consistent with the fluctuations in the boundary layers on the vehicle surface. These vortices persist until about $T = 10$ to $T = 20$, before the large-scale wake structures become dominant.

At this point some comment needs to be made on the pressure variation in the vehicle wake. Sims-Williams *et al.* (2001) show pressure contours in the wake of the vehicle and the trailing longitudinal vortex system can be clearly seen. Quinn *et al.* (2001) measured wind- and traffic-induced forces on portable road signs. These signs are normally placed at about one vehicle width away from the traffic, i.e., at $y/h = 1{\cdot}0$. It was found that the traffic-induced forces on these signs were solely due to a rapid change in pressure as the vehicles passed, and there was no evidence of forces caused by air movement. This indicates that disturbed pressure fields in wakes and slipstreams extend to greater distances from the vehicles than the velocities induced by passing vehicles.

It thus seems that there are some common characteristics of the near-wake flow of a wide range of different ground vehicles. The separated shear layers from the vehicle have a characteristic oscillation frequency $F$ of around 0·5 (within wide limits). These shear layers surround a reversed flow region immediately downstream of the vehicle. This oscillation decays along the wake, and a lower frequency oscillation with a value of $F$ of around 0·05 becomes dominant, at least for some vehicle types. This lower frequency oscillation is either due to a "pumping" of the reverse flow region immediately behind the vehicle (for blunt squareback cars), or a characteristic frequency of the entire wake structure. Downstream of the reversed flow region the wake of many vehicles contains longitudinal concentrations of vorticity, which are discernible to about $X = 5$ for the more streamlined shapes.

### 2.3. Far Wake

The measurements shown in Figures 1–4 for the wakes of a lorry and a high-speed train show that, in the far wake (defined as $T > 10$), for the measurement points nearest the models there is a gradual decay in ensemble-averaged velocities and standard deviations.

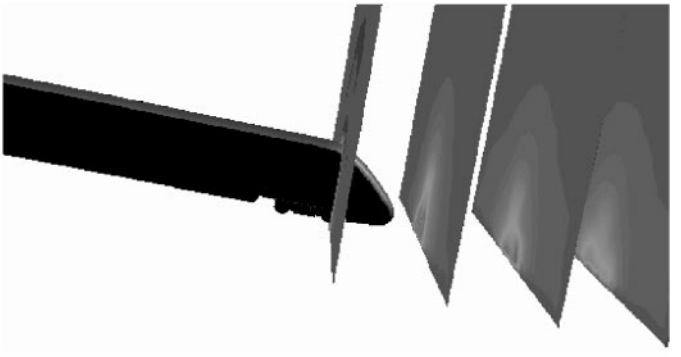

(a) Velocity predictions

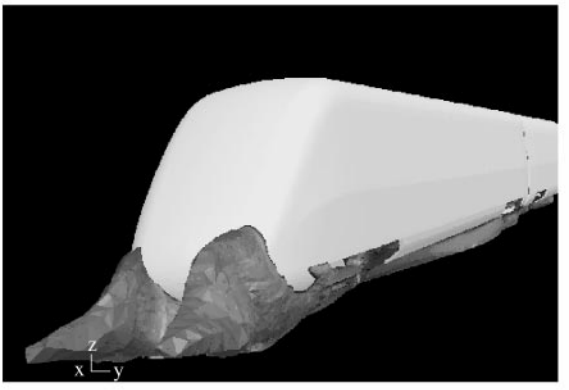


(b) Pressure isosurfaces

Figure 9. CFD calculations of train wake flows taken from Matschke & Heine (2000).

For those points furthest away from the vehicle models, the velocity first rises, as the disturbed flow field reaches the probe position, and then decays gradually. The wavelet spectra show a gradual decay in wavelet power down the wake, with most of the energy at nondimensional frequencies of around 0·03 to 0·1. It has been argued above that this frequency corresponds to a large-scale unsteadiness of the overall wake structure.

Now, Eskridge & Hunt (1979) carried out a detailed mathematical analysis of the far wake of vehicles. This has been taken further in the doctoral study of Hider (1998). Both studies present similar equations (although derived in different ways) for the longitudinal velocity component behind the vehicle and Hider goes on to derive formulae for the lateral and vertical components as well. These can in principle be compared with the results of Figure 1. The three velocity components are given by

$$U = \alpha \frac{Z}{T} \exp\left[ -\beta \frac{Y^2 + Z^2}{T^{0{\cdot}5}} \right], \quad V = \frac{\alpha}{2} \frac{YZ}{T^2} \exp\left[ -\beta \frac{Y^2 + Z^2}{T^{0{\cdot}5}} \right], \tag{1, 2}$$

$$W = \frac{\alpha}{2} \frac{Z^2}{T^2} \exp\left[ -\beta \frac{Y^2 + Z^2}{T^{0{\cdot}5}} \right]. \tag{3}$$

Here $U$, $V$ and $W$, are respectively, the dimensionless wake velocities in the longitudinal, lateral and vertical directions, and $\alpha$ and $\beta$ depend upon a number of parameters within the model. The value of $\alpha$ is given by $1/\gamma$, where $\gamma$ is the dimensionless eddy viscosity, and $\beta$ is

given by $1{\cdot}61/\gamma^{0{\cdot}5}C_D^{0{\cdot}5}$ for a vehicle with its height equal to its width, where $C_D$ is the vehicle-drag coefficient. These expressions have been derived from the fundamental assumptions that the wake-velocity profiles have a self-preserving form, and that the eddy viscosity in the wake is constant at any one cross-section and scales on the maximum velocity and the size of the wake at that section. In making a comparison with the experimental results, it needs to be remembered that the results of Figure 1 actually show the effective dimensionless velocity measured by the hot wire probes. These are the vector sum of the velocities in the vehicle direction of travel, and, for the probes at the side of the vehicle, the horizontal velocities normal to the direction of travel. The above expressions can be used to obtain the following expression for this velocity:

$$U' = \alpha \frac{Z}{T}\left(1 + \frac{Y^2}{4T^2}\right)^{0{\cdot}5} \exp\left[ -\beta \frac{Y^2 + Z^2}{T^{0{\cdot}5}} \right]. \tag{4}$$

However, in the far wake, $Y \ll T$, and equation (4) reverts to the simpler form of equation (1), and $U' = U$ with little loss in accuracy. It is thus possible, by fitting equation (1) to the data of Figure 1, to obtain best-fit values of the constants $\alpha$ and $\beta$. If the form of the above equation is correct, then these values should be constant across the wake. The work of Eskridge & Hunt (1979) assumes that $\gamma = 0{\cdot}4$ (the von Karman constant) and $C_D = 0{\cdot}35$. These values give $\alpha$ and $\beta$ equal to 2·5 and 4·3, respectively, for the wakes of the cars that they studied. The results of the curve fit are shown in Figures 10 and 11. In Figure 10 results are given for three different distances of the probe from the vehicle side. The agreement can be seen to be good, and the predictions seem to have the correct form. However, the results of Figure 11 show the best fit values of the constants are not constant across the wake, but show considerable deviation at the outer edge. This suggests that the fundamental assumption of self-preserving velocity profiles is not wholly valid in this case, perhaps due to the

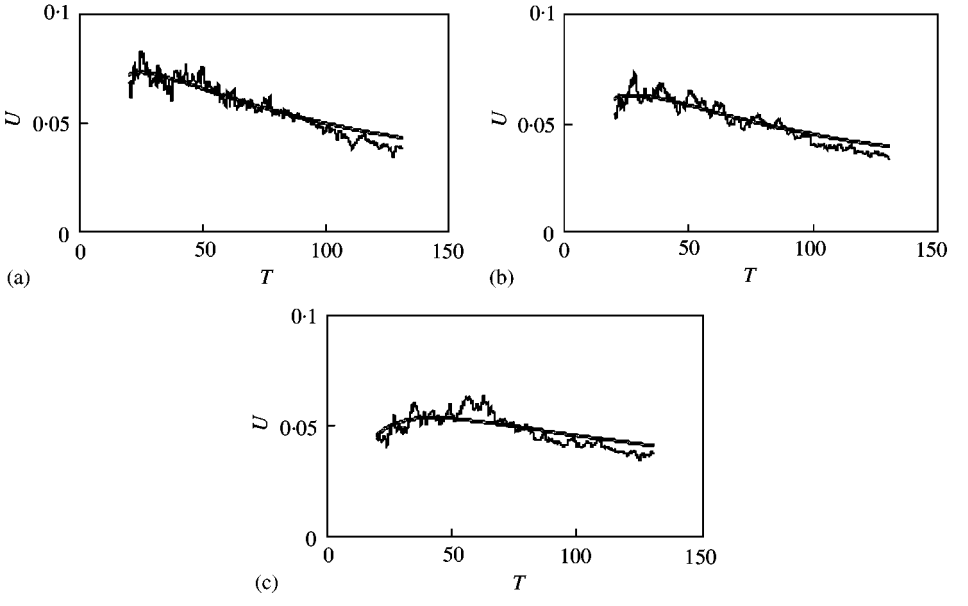


Figure 10. Fits of theory of Eskridge & Hunt (1979) to train wake data at (a) $y/h = 0{\cdot}033$, (b) $y/h = 0{\cdot}1333$, (c) $y/h = 0{\cdot}40$. (See Figure 1 for details of experimental results. Solid line represents best fit of equation (4) to experimental data.)

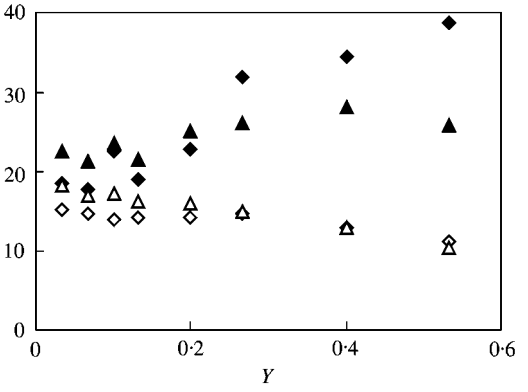


Figure 11. Curve-fit parameters $\alpha$ and $\beta$ for fits of theory of Eskridge & Hunt (1979) to lorry and train wake velocity data: ◆, $\alpha$ for lorry; ◇, $\beta$ for lorry; ▲, $\alpha$ for train; △, $\beta$ for train.

large effect of the separated shear layers which, it should be noted, are of the order of 0·5 h at the separation position, i.e., far from negligible in terms of the wake size (Baker *et al.* 2000, 2001). This lack of similarity was also noticed in the work of Eskridge & Thompson (1982) who carried out velocity measurements in the wake of a block shape held above a moving ground plane. They attempted to find a better velocity formulation by allowing different scaling lengths in the lateral and vertical directions, and arrived at an expression similar to equation (1), except for the appearance of the ratio of vehicle height to vehicle width as a multiplier to the equation. For the cars that they were studying this improved the agreement between experiment and theory, but for the lorry and train model considered here, for which the width/height ratio is close to 1, the effect would be small. They also attempted to improve the fit by allowing the theoretical eddy viscosity to vary with height. Whilst an improved fit was obtained, it was at the expense of simplicity, and a numerical solutions to the problem were required. Note also from Figure 11 that the measured value of $\alpha$ is much higher than that predicted by Eskridge & Hunt, suggesting that the eddy viscosity is significantly lower. This effect of the lower eddy viscosity also results in an increased value of $\beta$ although this is to some extent compensated for by a higher drag coefficient for the train and the lorry than that used by Eskridge & Hunt for a car.

Eskridge & Hunt (1979) also give expressions for the three components of turbulence in the far wake of vehicles, on the assumption that the principle of self-preservation also holds for the turbulence profiles. The solution required values of a number of experimental constants to be determined from experimental data. However, Eskridge & Thompson (1982) show that the scaling lengths for the turbulence profiles were different from the velocity profiles, and derived another set of formulae, which again required experimental data to determine some constants. In particular, the form of the lateral and vertical variation of turbulence had to be obtained from experimental data. Now the experimental data of Figure 3 for the standard deviations of the ensemble time histories should give some indication of wake turbulence. However, they do not allow the various expressions for turbulence intensity to be evaluated since they represent a complex combination of both the longitudinal and lateral components of turbulence.

It can thus be seen that in the far wake, there is a gradual decay of the vehicle-induced velocity and turbulence, with a characteristic wake frequency of around 0·03–0·1. It can also be concluded that the theory of Eskridge & Hunt (1979) is a reasonably good description of the measured wake behaviour, provided suitable parametric values are chosen.

## 2.4. Cross-Winds and Topography

In this section, we will consider the effects of cross-winds and urban topography on the flow within vehicle wakes. The particular urban topography that we will consider will be the classical "street canyon" for which a wide body of literature exists.

It can be expected that the primary effect of a cross-wind, either in open terrain or within a street canyon, will be to translate the wake in the wind direction. Indeed, this is the primary mechanism assumed by Eskridge & Hunt (1979) and Hider (1998) for open terrain, and by Yamartino & Wiegand (1986) in their derivation of a model for street canyon flow. However, there will be other effects due to atmospheric turbulence. In open terrain, the integral length scale of atmospheric turbulence close to the ground is around 50–100 m, and wide variations in wind velocity can be experienced over a time scale of around 10 s. Now, the typical spanwise length scale of a vehicle wake can be expected to be of the order of 5 m, and a typical wake-time scale of the order of a second or so. Thus, in open terrain it can be expected that the vehicle wakes will firstly be "translated" in the direction of the wind and secondly will be significantly affected by atmospheric turbulence, largely by undergoing large scale "wafting" motions, but with some turbulent diffusion. Within a street canyon, the length scales and time scales of the wind will be smaller, and will approach those of the wake. In such circumstances, as well as translation of the wake, it is likely that there will be significant diffusion of the wake, as the main energy containing eddies within the flow will be at similar scales to the wake. In both cases, in anything other than weak wind conditions, the effects on wake flows will be substantial.

This having been said, let us now consider the effect of cross-winds on wake development in open terrain. We consider mainly the low wind speed case (with yaw angles less than 10–20°). The effect of high wind speeds on vehicle behaviour, which is primarily of importance in terms of vehicle safety, is fully described in Baker (1991a–c). Bearman *et al.* (1983) show that, for a car model at a yaw angle of around 10°, the longitudinal trailing vortex pattern becomes exceedingly complex, with a number of vortices of different strengths. Some of the results are reproduced in Figure 12. A number of investigators have studied the wake of a high-speed train at small angles of incidence (Mair & Stewart 1985;

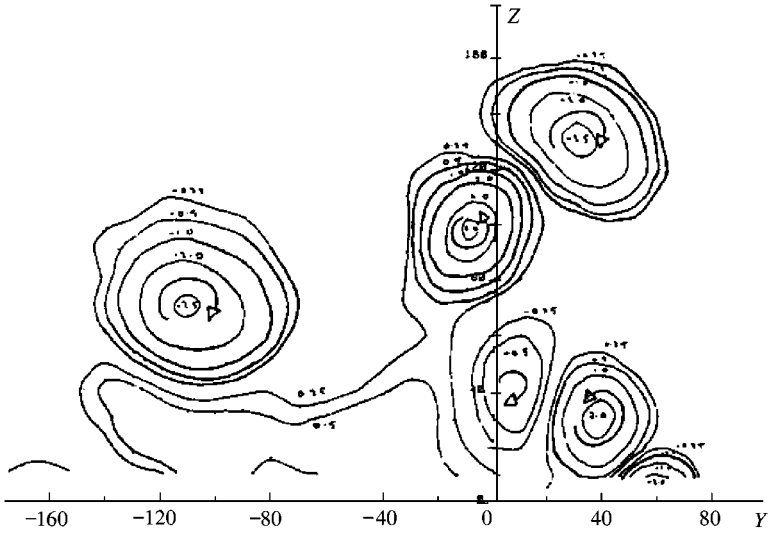


Figure 12. Vorticity in wake of wind tunnel car model at 10° yaw; taken from Bearman *et al.* (1983).

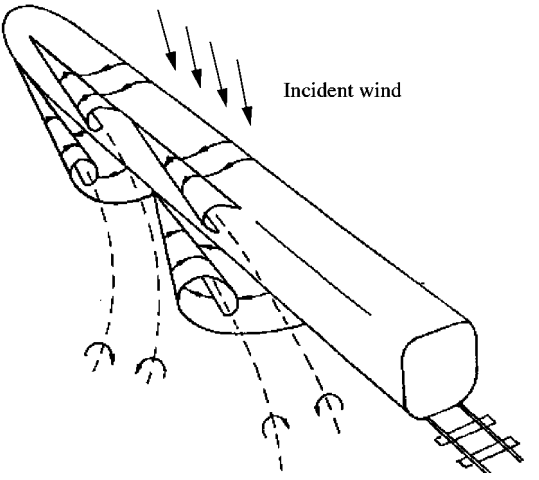


Figure 13. Sketch of vortex pattern in the wake of a train in a cross-wind; taken from Copley (1987).

Copley 1987; Chiu 1991; Robinson & Baker 1990). In such circumstances, a strong trailing vortex pattern forms on the leeside of the vehicle, which has many similarities to those found around an isolated slender body at yaw—see Figure 13. The different authors present detailed experimental results, and also describe methods for calculating the flow fields, based on panel methods with embedded vorticity. The effect of small levels of turbulence is to modify the strength of these vortices (Robinson & Baker 1990). For lorries and trains, the investigation of Baker *et al.* (2000, 2001) included measurements made with a simulated cross-wind, with a wind speed/vehicle speed ratio of 0·23, i.e., a yaw angle of 13°. The results of these measurements are shown in Figure 14, in a similar format to those of Figure 1. The probe rakes were placed on the leeside of the vehicle. It can be seen that the main effect is to considerably shorten the region behind the vehicle at which the wake can be discerned at the probe location—presumably because the wake is both disrupted and blown away from the track behind the vehicle. In fact the wake can only be discerned for $T < 15$. The second effect is to produce very high gust speeds in the very near wake of the model for the bluff lorry shape.

Now, let us consider the effects of street canyons on vehicle wake development. The classic definition of street canyon flows is given in Oke (1987). He classifies these flows based on the ratio of building height to canyon depth, as shown in Figure 15. The most frequently studied of these three configurations is the skimming flow case with a nominally trapped vortex within the canyon. Recent work by Louka *et al.* (1998, 2000) shows that the reality is considerably more complex than this figure suggests, with the vortex structures that were observed being highly intermittent, and the magnitude of the turbulence fluctuations being in many cases greater than the mean values. They postulate that the dominant flow structure is an unsteady shear layer at the top of the canyon, that induces an unsteady circulation within the canyon. As mentioned above, since the size of vehicle wakes will be of the same order as the size of the turbulent eddies within a canyon, it is to be expected that the wakes will be considerably disrupted in such circumstances. Kastner-Klein *et al.* (1999) present comprehensive wind tunnel data for the velocity and concentration fields within street canyons, with and without a simulation of moving traffic conditions. They show that the effect of vehicle movement on the cross canyon flow velocities is insignificant, but that the cross canyon turbulence intensity could increase by 0·1 in the upwind corner of the canyon. The along canyon flow velocities were, however, considerably affected. The nature

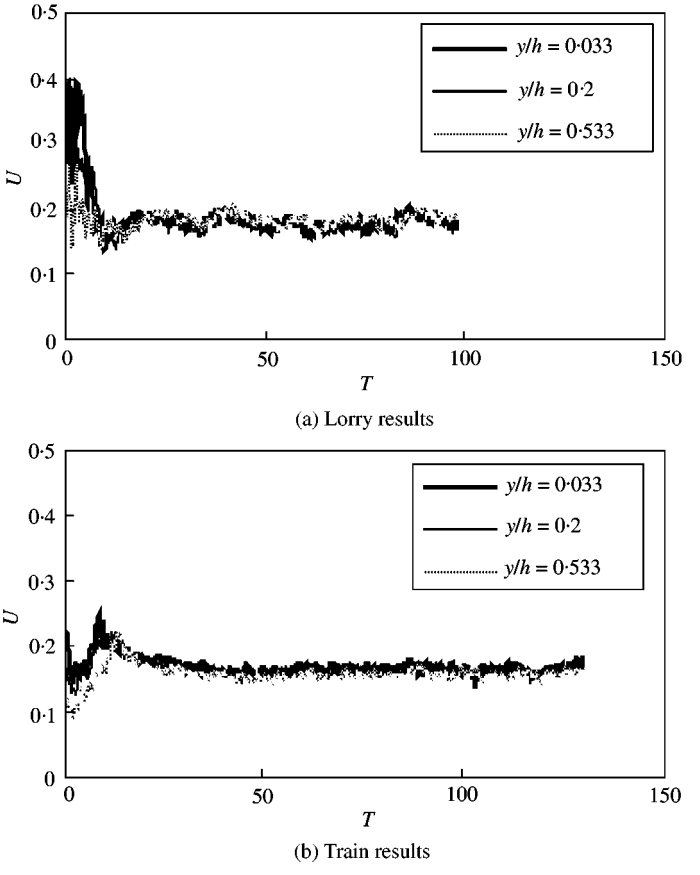


Figure 14. Effect of cross-wind on ensemble averaged wake velocities of lorry and train models on moving model rig. (Velocities measured with hot films mounted at model mid height in horizontal line normal to the vehicle side on the lee side of the model, nominal model speed of 30 m/s. Wind normal to vehicle direction of travel with mean speed of 6·8 m/s. See Baker *et al.* (2000, 2001) for experimental details.)

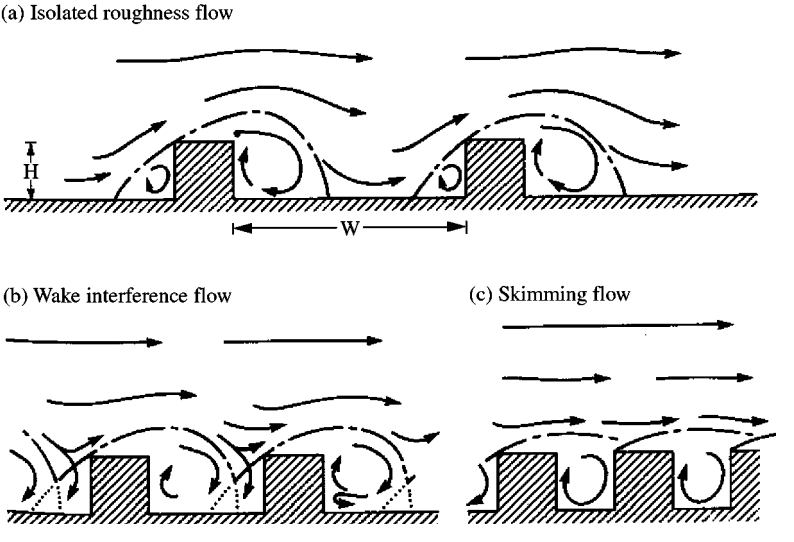


Figure 15. Street canyon flow fields; from Oke (1987).

of this effect depended upon whether one-way or two-way traffic was simulated. With two-way traffic, there was little change in the mean velocity, but a significant increase in the along canyon turbulence intensity in the upwind corner of the canyon of up to 0·2. With one way traffic there was a considerable along-canyon velocity induced, but with a rather lower increase in turbulence intensity.

Thus, it can be seen that in general the available experimental data support the hypothesis that the effect of cross-winds is to translate and diffuse the vehicle wake, with the diffusion process being more dominant within street canyon topography. However, more experimental measurements of wake development in cross-winds are required to fully define the velocity fields within wakes affected in this way.

## 3. DISPERSION IN VEHICLE WAKES

### 3.1. Near Wake

The experiments described by Richards *et al.* (2000a, b) give some indication of the dispersion of pollutants in the near wake of a fastback car. These measurements were made using fast response Flame Ionisation Detectors at various points within the near wake of the vehicle. Figure 16 shows a typical time history of concentration measured at $X = 0{\cdot}42$, $Y = 0{\cdot}31$ and $Z = 0{\cdot}36$. The "peaky" and intermittent nature of the time histories are very apparent. Figure 17 shows the concentration distributions across the wake at this section, as measured and as predicted from a nonlinear $k$–$\varepsilon$ CFD calculation. It is of interest to see that the experimental results show a peak of concentration near the top of the vehicle, where the exhaust has been entrained in the upper portion of the two-tier separation region. The CFD calculations do not predict this two-tier structure in the separation region (Section 2.2), and are thus unable to predict the elevated pollutant concentrations in the upper levels of the wake. Figure 18 shows the concentration spectra at various distances downstream of the vehicle at $Y = 0{\cdot}31$ and $Z = 0{\cdot}36$. At the measurement points closest to the vehicle there can be seen to be two peaks—one at a value of $F$ of 0·3 and one at a value of 1·0. The lower peak probably corresponds to a very low-frequency wake oscillation that was observed visually by the investigators, that involved a low-frequency purging of the pollutant in the wake. The higher frequency peak probably corresponds to oscillations of the separated shear layers. At

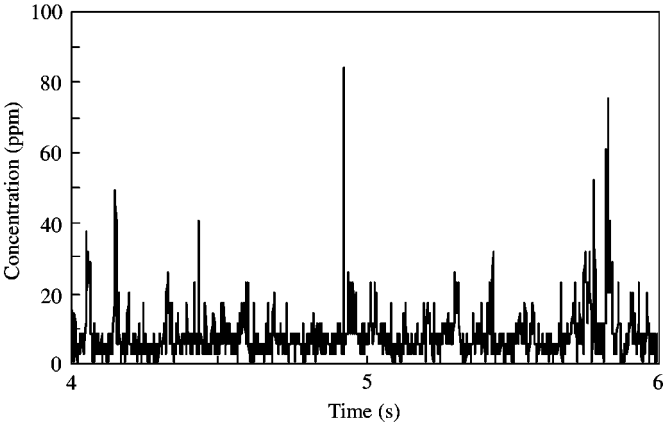


Figure 16. Pollutant concentration time history behind car. (Measurements made at $X = 0{\cdot}42$, $Y = 0{\cdot}31$ and $Z = 0{\cdot}36$. See Richards *et al.* (2000b) for experimental details.)

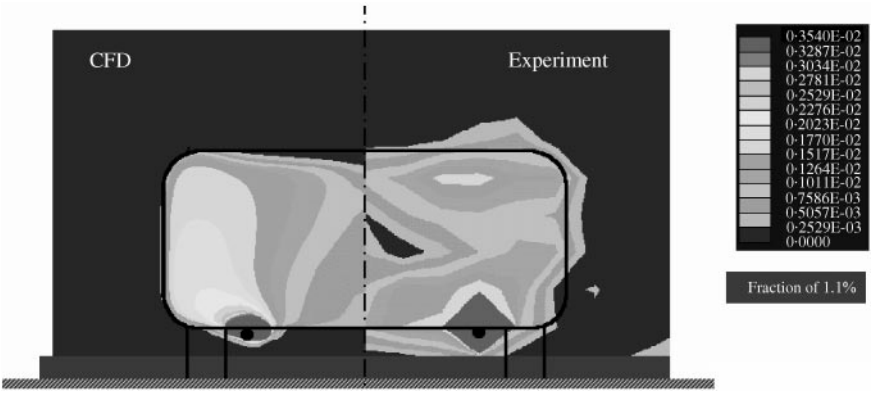


Figure 17. Pollutant concentration data at $X = 0{\cdot}42$ behind car model (Pollutant input from exhaust position shown. (CFD results on left, experimental results on right; results at $X = 0{\cdot}42$, wind speed = 13 m/s. CFD results were obtained with an upwind differencing scheme and a nonlinear $k$–$\varepsilon$ turbulence model. See Richards *et al.* (2000a, b) for further details.)

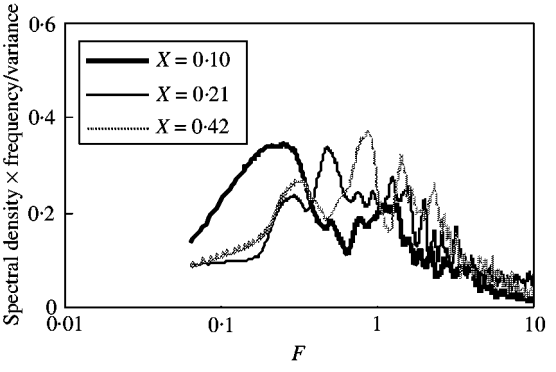


Figure 18. Concentration spectra in wake of car measured at $Y = 0{\cdot}31$ and $Z = 0{\cdot}36$ (see Richards *et al.* (2000b) for experimental details.)

$X = 0{\cdot}42$ the spectrum is very similar to the velocity spectrum at the same point shown in Figure 7. Thus, it can be seen that the pollutant concentration distribution basically follows the underlying velocity distribution. More data are, however, required for different vehicle types.

### 3.2. Far Wake

The investigation of the nature of dispersion in the zero cross-wind case has largely concentrated on the development of analytical models, and a comparison of these models with the little wind-tunnel and full-scale data that exists. The major work in this field was carried out in the late 1970s and early 1980s by Eskridge and his co-workers (Eskridge & Hunt 1979; Eskridge *et al.* 1979; Eskridge & Rao 1983, 1986), and is based on the velocity profile descriptions set out in Section 2.4. Pollutant dispersion was incorporated in this using an equation for pollutant conservation, and concentration profiles downstream of the vehicle were calculated. The latter work of Eskridge & Rao (1986) used the corrected velocity profiles of Eskridge & Thompson (1982). A similar approach was adopted by Hider

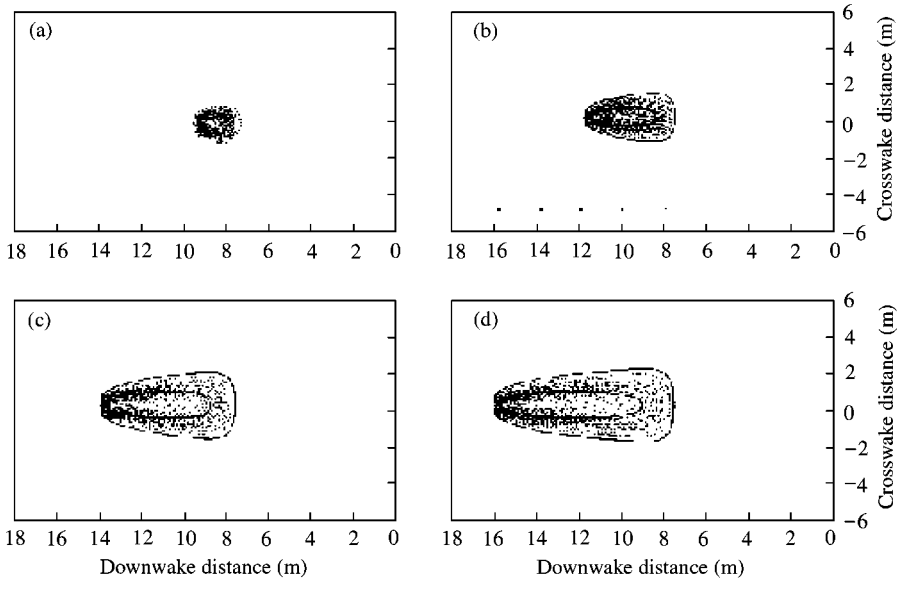


Figure 19. Concentration contour plots in wake of car at $Z = 0{\cdot}25$. Calculations made using the analysis of Hider (1998). The vehicle is travelling from right to left at a speed of 15 m/s. The concentration plots are at dimensionless times $T$ of (a) 1·5, (b) 3, (c) 4·5 and (d) 6. Pollutant is emitted from the end of the near wake at $Z = 0{\cdot}25$.

(1998), but she adopted a different, more efficient, numerical scheme for the solution of the equations. Typical results are shown in Figure 19. This shows the lines of constant concentration as pollutant leaves a vehicle of height 1·5 m moving at a speed of 15 m/s, over a 0·6 s period. The origin of the concentration plume should be regarded as being at the start of the far-wake region (i.e., $T = 10$) since the calculation is only valid in this region. A time of 0·6 s thus corresponds to a value of $T = 6$ from the start of the far wake. The dispersion of the plume as the vehicle moves away from its starting point can be clearly seen.

Hider also studied the dispersion of particulate material in the vehicle wake, again using the velocity field outlined in Section 2.4. The particles were assumed to be advected by the flow, and to settle under their own weight. A dispersion model was also incorporated, based on the random walk model of Nalpanis *et al.* (1993). Typical particle trajectories are shown in Figure 20(a), for the same conditions as in the last paragraph, and the turbulent diffusion about the mean flow direction can be clearly seen. Figure 20(b, c) shows the effect of different release heights and particle diameters, on the landing position of a cloud of particles. The thing that is most apparent from these results is the length of a typical particle trajectory. For the smallest particles that were considered (20 $\mu$m) these are of the order of 150 m when released at $Z = 0{\cdot}25$ and 500 m when released at $Z = 1$. Clearly, such particle lengths mean that in a practical situation particulate pollutants would interact with the wake of other vehicles, and might thus be expected to stay in suspension for very long periods indeed.

### 3.3. Cross-Winds and Topography

Paradoxically, there is considerably more experimental information available on the nature of pollutant dispersion in vehicle wakes in cross wind conditions and in urban street canyons than for the simpler no cross-wind case, probably because of the greater practical

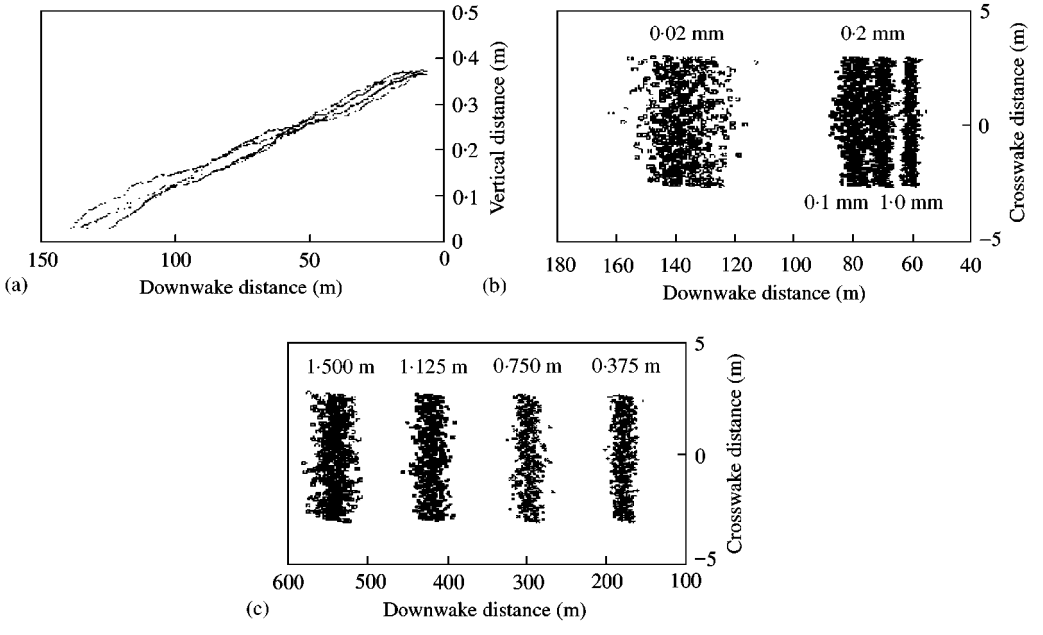


Figure 20. Movement of particles in vehicle wakes (Results obtained using the analysis of Hider (1998). Vehicle is travelling at 15 m/s and has a height of 1·5 m; (a) shows typical particle trajectories for a release height of 0·375 m and particle diameters of 20 μm. (b) shows the landing positions of particles of different sizes, relative to the car for a release height of 0·375 m, and (c) shows landing positions for different particle release heights with a particle diameter of 20 μm.)

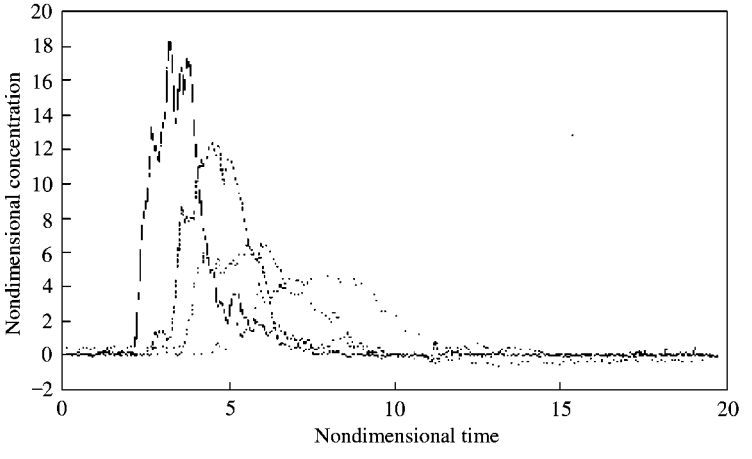


Figure 21. Ensemble average concentration time histories downwind of an isolated lorry model on a moving model rig from Baker & Hargreaves (2000). (The ratio of wind-tunnel speed to vehicle speed was 0·54. The measurements were made at $Y = 1{\cdot}6$, 3·2, 4·8 and 6·4 with $Z = 0{\cdot}5$. The $Y = 1{\cdot}6$ curve is the one that peaks first and so on. Full experimental details, including details of the atmospheric boundary layer simulation are given in Baker & Hargreaves (2000).)

importance of such cases. Hargreaves and Baker (2001) present results for the dispersion in the wake of an individual vehicle model (of a lorry) as it is fired across a wind tunnel in which an atmospheric boundary layer has been simulated, for both the open terrain and street canyon case. It was found that for each pass of the model across the wind tunnel, the measured concentration time histories could vary significantly. To enable stable readings to

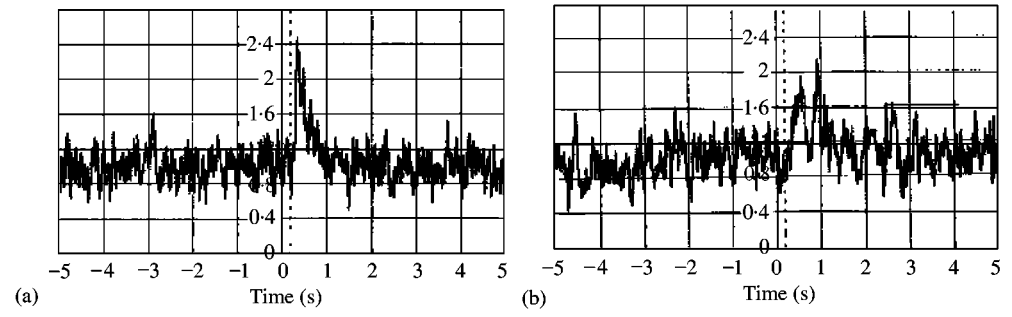


Figure 22. Ensemble average time histories of concentration showing effect of moving vehicles taken from Pearce & Baker (1997). (Experiments were carried out in a street canyon simulation of height/width ratio of 0·45. The models were in trains of four, separated by two vehicle heights. The measurements in Figure 23(a) were made on the upwind side of the canyon, 3·3 heights above ground level and those in Figure 23(b) on the downwind side of the canyon at the same height.)

be obtained, ensemble averages of the data were formed. Typical values are shown for the open terrain case in Figure 21. It can be seen that the concentration increases and then decreases as expected. As the measuring point moves further away from the vehicle the peak value decreases and the time to peak increases. In the street-canyon case (not shown) there is some evidence for a secondary peak, which is associated with the recirculation in the street canyon. The time scales of these concentration slugs will be determined by both the time scales inherent within the wake, and those of the flow within the street canyons. For the open terrain case the dimensionless time scale of the pollutant rise and fall (based on vehicle length) is around 5. For the street-canyon case, it is around 20. If these are expressed in terms of vehicle heights, these values become around 15 and 60, respectively, which are not inconsistent with the overall wake time scale mentioned in Section 2.3.

Pearce & Baker (1997) also describe moving model experiments, but these were carried out in a rather different manner, with single and multiple vehicles being fired along a wind tunnel model of a street canyon with a simulated cross-wind, in which tracer gas was released from the floor of the wind tunnel as a line source along the length of the canyon. Again ensemble averaging of the results of individual passes of the models had to be used to obtain stable results. It was found that the effect of the passage of one vehicle did not seem to affect the concentration field, but that a four vehicle train did produce a noticeable effect. This is illustrated in Figure 22(a, b) for the upstream and downstream sides of the street canyon. An increase can be seen in concentration associated with vehicle passing, that is most significant on the upstream side of the canyon. This is the direction in which the wake would be translated by the canyon flow, and possibly represents some concentration of the pollutant by the near-wake flow of the vehicle. The dimensionless duration of these events, based on vehicle height is around 50.

The velocity measurements of Kastner-Klein *et al.* (1999) have been mentioned above. The measurements also made to assess the effect of moving vehicles on pollutant concentrations, with pollutant released from a line source in a similar manner to Pearce & Baker. They showed that for two-way traffic there was little effect of traffic movement on the concentration field (which is consistent with the small velocity changes that were measured). For one-way traffic there was a significant increase in concentration in the upwind corner of the canyon, which was again consistent with the velocity measurements.

Modelling of the concentration field in cross-wind conditions has been carried out by Hider (1998), based on the work of Eskridge *et al.* (1979), but with rather different numerical

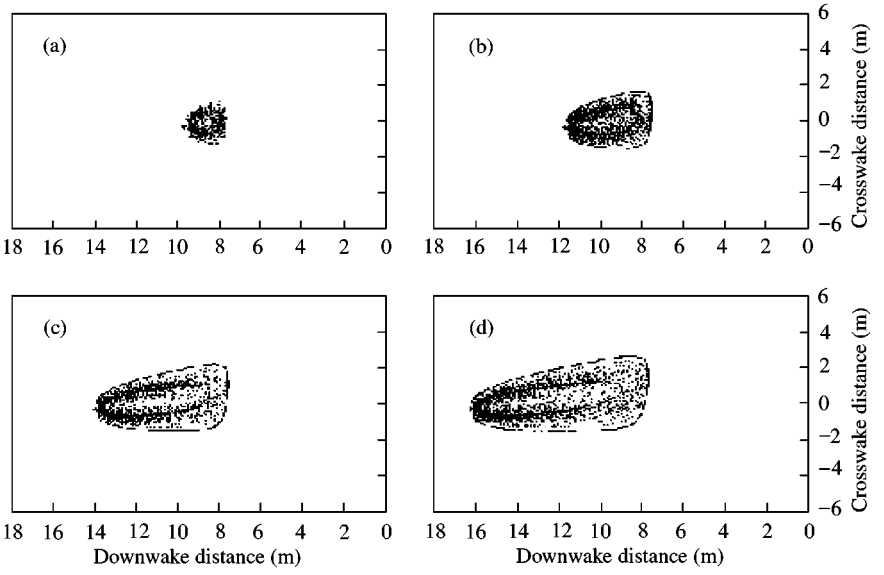


Figure 23. Concentration distributions from vehicle with weak cross wind (Calculations made using the analysis of Hider (1998)). The vehicle is travelling from right to left at a speed of 15 m/s. The concentration plots are at dimensionless times $T$ of (a) 1·5, (b) 3, (c) 4·5 and (d) 6. Pollutant is emitted from the end of the near wake at $Z = 0{\cdot}25$.)

schemes. Typical results are shown in Figure 23 for the release of a tracer from the end of the near wake of the car. The calculation parameters are identical to those of Figure 18. The skewing of the plume is very obvious.

Baker (1996) considered the case of a general vehicle in a cross-wind. He divided the wake of the vehicle into near-wake and far-wake regions, with the extent of the near-wake region varying with wind direction (from 20 vehicle heights at 5° yaw to 1 vehicle height at 90° yaw). The velocities in the near wake were assumed to decrease in a power law manner, based on the results of Eskridge & Hunt (1979). There is an inconsistency here in that the assumed decays are only truly valid for the far-wake region. At the end of the near wake, pollutant is taken to be emitted into the wind field as a series of Gaussian puffs, which then diffuse under the action of atmospheric turbulence. This approach is simple and can be faulted in places, but it does allow analytical formulae for concentration levels downwind of roadways to be derived, that give some insight into the physical mechanisms involved. For example, for a stream of fast moving vehicles ($N$/h) on a roadway with a neutrally stable cross-wind, the concentrations near to the road are given by

$$C = 6{\cdot}96 \times 10^{-4} \frac{NQ}{hw^{2/3}u^{4/3}}, \tag{5}$$

where $Q$ is the emission from a single vehicle, $h$ is the vehicle height, $u$ is the vehicle speed, and $w$ is the wind speed. Now it is known that the discharge $Q$ varies significantly with vehicle velocity and whilst the above formula would suggest that concentrations fall as vehicle speed increases, an increase in $Q$ with vehicle speed may nullify this effect.

Hargeaves & Baker (1997) describe a similar but rather more complex model, again based on the dispersion of Gaussian pollutant puffs. It is essentially a transient model and allows different time histories of vehicle speed, vehicle density, wind speed, etc. to be included, and

can be run for either the open-terrain or street-canyon case. The puffs move and diffuse under the influence of the ambient wind speed, given by either a logarithmic law in the open terrain case, or the model of Hotchkiss & Harlow (1973) for the street-canyon case, and a superimposed vehicle wake velocity, given by the expressions of Eskridge & Hunt (1979). Baker & Hargeaves (2000) describe some moving model wind-tunnel tests to validate this approach. As pointed out above, the results of individual moving model runs varied widely because of the relative size of the wind-tunnel turbulence to the wake size, and ensemble averages were required to produce stable concentration time histories. For the sake of consistency the model was validated by forming ensemble averages of a number of model runs with ARMA-generated wind fields, with the correct overall spectral characteristics. The model was shown to perform well in the open terrain case, but did not really represent the wind-tunnel results well in the street canyon case.

It can thus be seen that various methods exist for predicting the dispersion of pollutants in vehicle wakes in complex cross-wind and topographical conditions, and that these have been broadly validated by comparison with wind-tunnel and full-scale measurements. However, there seems to be a lack of reliable experimental data for relatively simple conditions that would enable these models to be more fully validated and their various components properly investigated.

### 3.4. The Full-Scale Context

The previous sections have considered the velocity fields and pollutant dispersion in the near wakes and far wakes of vehicles. The question now arises as to the utility of this work in the specification of the dispersion of pollutants from road vehicles in practical situations. In beginning to answer this question, it is instructive to consider the nature of time histories of pollutant concentration. Figure 24 shows data for PM10 concentrations (particulate matter with diameters less than 10 $\mu$m), as measured by the U.K. Department of the Environment in the centre of Nottingham, U.K., during 1998, supplemented by data from the experiments of Namdeo *et al.* (1999) for a site in the outskirts of Nottingham. Figure 24(a) shows the average weekly data during 1998, from the National Air Quality Archive web site (NAQA 2000). Figure 24(b) shows the same data for mean daily concentrations between January and March 1998, and Figure 24(c) shows the data for mean hourly concentrations over the two-week period in January 1998. It can be seen that there are certain systematic fluctuations in the data—the lower levels in the summer period (around 25–35 weeks) reflect the lower traffic levels during the holiday periods for example. A strong weekly period of fluctuation, due to the weekly traffic cycle, and a similar one day cycle that shows the effect of weekday peak periods can be seen quite clearly. There is also considerable random variation that is caused by large-scale weather systems passing over the site. At the hourly level there can be seen to be considerable fluctuations in the measured concentrations, presumably due to small-scale meteorological effects. Figure 24(d) shows the data of Namdeo *et al.* for 27/1/98 and 28/1/98 plotted at 1 min intervals over a 1 day period. The peak hour effect is again obvious, but the random peaks are also becoming of more significance. Finally, Figure 24(e) shows the data of Namdeo *et al.* plotted at 6 s intervals for the hour between 8·30 am and 9·30 am on 27 January 1998. The peakiness and randomness of the data is very apparent at this scale.

From what has been said in previous sections, it is apparent that the time scales of fluctuations of velocities and concentration distributions in the wake of ground vehicles is of the order of $T = 2$ for near-wake oscillations associated with shear layer unsteadiness, and around $T = 20$ for an oscillation that affects the entire wake system, which may arise from a variety of effects and can for some vehicles be associated with an axial pumping at the end

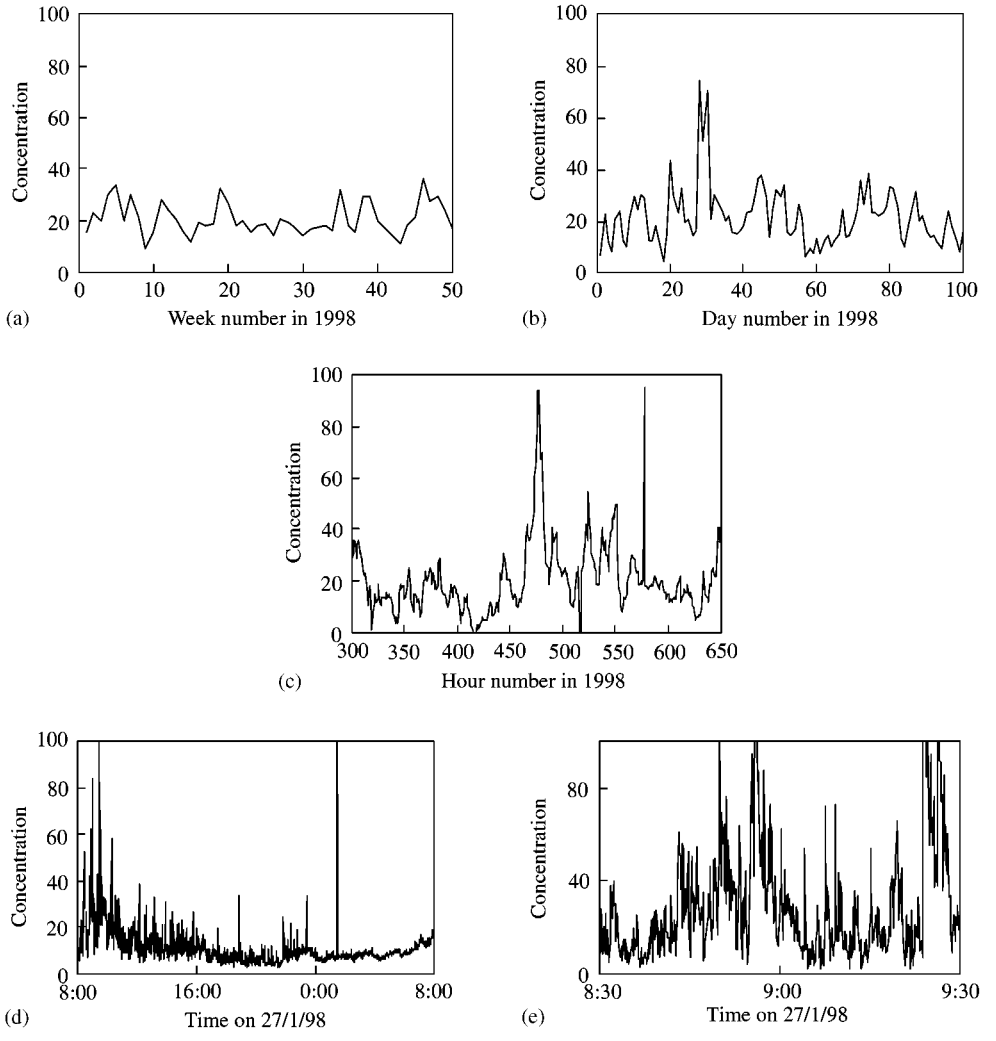


Figure 24. Time series of PM10 concentrations in Nottingham in 1998 (data taken from DOE (2000) and Namdeo *et al.* (1999). Concentrations in $\mu g/m^3$.)

of the near-wake recirculation region. Now, for typical full-scale values for large vehicles with a height of 3 m, moving at 15 m/s, these figures correspond to times of around 0·4 s for the low-period fluctuation to values of around 4 s for the large period fluctuations. Duell *et al.* (1999) give a full-scale equivalent for the "wake pumping" fluctuations of squareback cars of about 1 s. Thus the time scales of vehicle wake unsteadiness are likely to be around 1 s—rather more rapid than the time scale of the fastest fluctuations identified in Figure 24.

Now, in general, legislative requirements mean that pollutant dispersion models need to predict peak pollutant concentrations over 15 min. or 1 h periods. Whilst this is at first sight sensible, the large peaks in Figure 24(e) over 6 s periods and the vehicle wake peaks at around 1 s period must give some cause for concern. What is important in physiological terms is the pollutant dose absorbed by pedestrians, and these large peaks, at periods close to the period of the breathing cycle, may well be of significance. In other words, if a breath is taken as one of these short-term peaks passes, then the pollutant dose could be very high

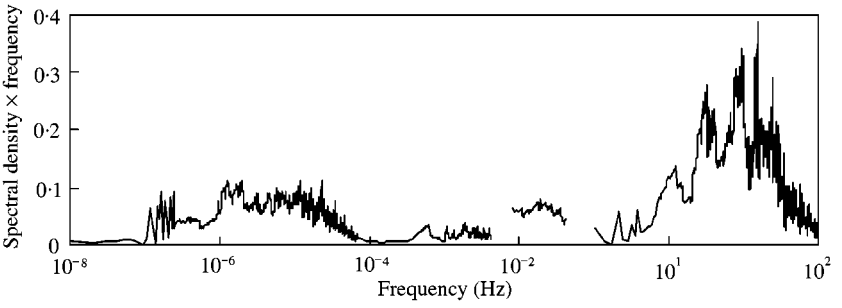


Figure 25. Spectra of pollutant concentrations (data taken from DOE (2000) for frequencies $<10^{-4}$ Hz, from the data of Namdeo *et al.* (1999) for frequencies between $10^{-4}$ and $10^{-1}$ Hz and from data of Richards *et al.* (2000b) for higher frequencies.)

indeed. This argument is particularly pertinent, where the pollutant is not rapidly removed from the body or bloodstream—for example small particulate matter is retained in the passages of the lungs for a considerable period.

In the light of the above, there can be seen to be two levels at which the vehicle wake and dispersion data could be used in pollution dispersion models—at a simple level and at a sophisticated level. At a simple level, these data could first be used to specify the geometry of the source term used in such models to simulate traffic emissions—what is its size, and how are the concentrations at the edge of the source term related to vehicle emissions? Secondly, these data could also be used to specify the average velocity and turbulence field in such models outside the immediate vicinity of the effective source term. Many models assume a model of pollutant dispersion based upon advection of the wake by the mean flow and dispersion of the plume through dispersion parameters that are proportional to the turbulence level, and usually the turbulence caused by traffic is calculated from empirical expressions from only very limited experimental data. Also, the length scales and time scales of wake turbulence are not usually considered in these calculations, although it is clear that these scales will largely determine the nature of the wake interaction with ambient conditions, and thus the dispersion of pollutants. The unsteady flow measurements outlined here allow the effect of turbulence energy at different scales to be properly considered.

At the more sophisticated level the data presented in this paper could be used to gain an understanding of the large peak fluctuations of pollutant that can be seen in the results of Figure 24(e). Figure 25 shows a composite spectrum of pollutant concentrations over a very wide frequency range, from the results of NAQA (2000), Namdeo *et al.* (1999) and Richards *et al.* (2000b). To give a degree of consistency the portion of the spectrum from each set of data has been normalised by its mean concentration squared, and the model scale results of Richards *et al.* have been converted to equivalent full scale values. This procedure seems reasonable, but the discontinuities in the curve of Figure 25 show that it has not been completely successful. Nonetheless the results are interesting. The various peaks in the spectra correspond to the various traffic and wind fluctuations mentioned above for frequencies less than 0·1 Hz. At the higher frequencies there can be seen to be a great deal of fluctuating energy due to fluctuations in the vehicle wake. In particular, there is significant energy at around 1 Hz, corresponding to a period of 1 s. If the above argument is accepted, then the fluctuations at this frequency could have a significant effect upon the doses of pollutants received by pedestrians. Clearly, more work is required here to identify just what the actual pollutant dose is, due to these very large, short-term peaks, and how these large peak concentrations should be defined, and over what period. Some sort of extreme value analysis of the type used in wind loading calculations may be appropriate here.

## 4. CONCLUDING REMARKS

From the work described in the preceding sections the following conclusions can be drawn.

(a) The wake of vehicles can be conveniently divided into a near-wake region up to 10 vehicle heights downstream of the vehicle trailing edge, and a far-wake region beyond that.

(b) The near-wake region is characterised by large-scale flow structures, usually consisting of a recirculation region and concentrations of longitudinal vorticity. The far-wake region is characterised by a gradual decay in wake velocities.

(c) In the near-wake flow a number of different unsteady flow mechanisms can be discerned at a variety of frequencies. An instability associated with the separated shear layers from the vehicle surface contains most of its energy at a nondimensional frequency $F$ of around 0·5–1·0. This particular flow mechanism persists further downstream as the rear of the vehicle becomes more streamlined. A lower frequency oscillation can also be discerned for some vehicles at a value of $F$ of around 0·05–0·1. This is either associated with the mechanism of wake pumping, or with a large-scale instability of the complete wake structure.

(d) In the far wake of the vehicles that were investigated there is no evidence of any instability due to the shear layer fluctuations, and the majority of the fluctuating energy is at scales associated with an overall instability of the vehicle wake. In this region, the mean velocity profiles can be reasonably represented by the theoretical formulation of Eskridge & Hunt, albeit with significantly different constants than those suggested in that theory.

(e) The effect of cross-winds on vehicle wakes, in both open terrain and in urban situations, is to translate the wake away from the vehicle direction of travel, and to diffuse the wake either through the "wafting" of the wake by large turbulent eddies, or by the diffusion of the wake due to smaller turbulence scales. A consideration of turbulence scales leads to the conclusion that diffusion of the wake by small-scale turbulence will be more important in the street canyon (urban) situation.

(f) There is little experimental information on the dispersion of pollutants within the near wake of vehicles but such as there is suggests that, very broadly, the pollutant concentration field mirrors the velocity and turbulence fields, and concentration fluctuations can be observed that are consistent with the fluctuations in the velocity field. The time histories of concentration have a "peaky", intermittent nature.

(g) Again, there is little information available on dispersion in the far wake of vehicles, but a number of analytical approaches exist. One point of interest to emerge from these is that particulate pollutants in the vehicle wake can be expected to settle a long way behind the vehicle.

(h) The effect of cross-winds and urban geometry on pollutant concentration fields from vehicles has been studied by a number of authors, experimentally, numerically and analytically, and the effects of traffic movement have also been investigated. To enable trends in the data to be observed when the pollutants from individual vehicles are studied, some form of ensemble averaging of the data is usually required. In general, the processes of pollutant translation and diffusion can be observed within vehicle wakes, in a manner that is consistent with the changes to the velocity and turbulence field.

(i) A consideration of pollutant concentration spectra at a wide variety of scales shows that a significant proportion of the overall variance of the fluctuations takes place at frequencies that are associated with wake fluctuations, and it is argued that these fluctuations (which have been shown experimentally can result in large peak values) can be of significance in determining pedestrian pollutant dose.

On the basis of the above conclusions, the following suggestions for further work can be made.

(a) Information on the size and intensity of vehicle near wakes needs to be incorporated into vehicle emission dispersion models, to define the initial boundary conditions for the calculations. This will require further information on the nature of the velocity and turbulence fields in the near wakes of a variety of vehicles.

(b) The dispersion of pollutants within vehicle near wakes also needs to be determined for a wider variety of vehicles than has been done to date, so that this data can also be used as input to pollutant dispersion models.

(c) Further experimental data are also required for the dispersion of pollutants in the far wakes of vehicles, to enable different analytical methods to be validated. These should be for simple geometric and topographical configurations, since the data that already exist are in general for situations with complex urban topography.

(d) The effect of short period concentrations (of the order of 1 s) of pedestrian pollutant on pedestrian dose rates (caused largely by fluctuations in vehicle wakes) needs to be investigated further, and integrated with physiological models of the breathing process.

## ACKNOWLEDGEMENTS

The author's initial interest in bluff body aerodynamics and vehicle aerodynamics first arose as a research student at the Engineering Department at Cambridge University in the late 1970s. David Maull played a significant role in arousing this interest. Also, it is clear from the above that this paper draws very heavily on the work of the author's students and his co-workers at the Universities of Nottingham, Birmingham, and elsewhere, and their names can be found in the list of references. Their hard work and stimulating suggestions and conversations are most gratefully acknowledged.

## REFERENCES

AHMED, S. R. 1981 Wake structure of typical automobile shapes. *ASME Journal of Fluids Engineering* **103,** 162–169.

BAKER, C. J. 1991a Ground vehicles in high cross winds—Part I: Steady aerodynamic forces. *Journal of Fluids and Structures* **5,** 69–90.

BAKER, C. J. 1991b Ground vehicles in high cross winds—Part 2: Unsteady aerodynamic forces. *Journal of Fluids and Structures* **5,** 91–111.

BAKER, C. J. 1991c Ground vehicles in high cross winds—Part 3: The interaction of aerodynamic forces and the vehicle system. *Journal of Fluids and Structures* **5,** 221–241.

BAKER, C. J. 1996 Outline of a novel method for the prediction of atmospheric pollution dispersal from road vehicles. *Journal of Wind Engineering and Industrial Aerodynamics* **65,** 395–404.

BAKER, C. J., DALLEY, S. J., JOHNSON, T., BROWN, M., GAYLARD, A., QUINN, A. & WRIGHT, N. G. 2000 Measurements of the slipstream and wake of a model lorry. *Proceedings of the MIRA Vehicle Aerodynamics Conference*, Rugby, U.K.

BAKER, C. J., DALLEY, S. J., JOHNSON, T., QUINN, A. & WRIGHT, N. G. 2001 The slipstream and wake of a high speed train. *Journal of Rail and Rapid Transport*, *Institution of Mechanical Engineers* — in press.

BAKER, C. J. & HARGREAVES, D. M. 2001 Wind tunnel evaluation of a vehicle pollution dispersion model. *Journal of Wind Engineering and Industrial Aerodynamics* **89,** 187–200.

BEARMAN, P. W. 1997 Near wake flows behind two- and three-dimensional bluff bodies. *Journal of Wind Engineering and Industrial Aerodynamics* **69–71,** 33–54.

BEARMAN, P. W., DAVIS, J. P. & HARVEY, J. K. 1983 Measurements of the structure of road vehicle wakes. I*nternational Journal of Vehicle Design*, Special Publication SP3, pp. 493–499.

BENSON, P. E. 1979 CALINE3 — a versatile dispersion model for predicting air pollutant levels near highways and arterial streets, Report FHWA/CA/TL–79/23.

BERKOWICZ, R., HERTEL, O., SORENSON, N. & MICHELSON, J. 1994 Modelling air pollution from traffic in urban areas. *Proceedings of the Institute of Mathematics and its Applications Conference on Dispersion through Groups of Obstacles*, Cambridge, U.K., pp. 121–141.

CHIU, T. W. 1991 A two-dimensional second-order vortex panel method for the flow in a cross wind over a train and other two dimensional bluff bodies. *Journal of Wind Engineering and Industrial Aerodynamics* **37,** 43–64.

COLEMAN, S. A & BAKER, C. J. 1994 An experimental study of the aerodynamic behaviour of high sided lorries in cross winds. *Journal of Wind Engineering and Industrial Aerodynamics* **53,** 401–429.

COPLEY, J. R. 1987 The three dimensional flow around railway trains. *Journal of Wind Engineering and Industrial Aerodynamics* **26,** 21–52.

DUELL, E. G. & GEORGE, A. R. 1992 Unsteady near wake flows of ground vehicle bodies. AIAA paper 92–2641.

DUELL, E. G. & GEORGE, A. R. 1993 Measurements in the near wakes of some ground vehicle bodies. SAE paper 930928.

DUELL, E. G. & GEORGE, A. R. 1999 Experimental study of a ground vehicle body unsteady near wake. SAE paper 1999–01–0812.

ESKRIDGE, R. E. & HUNT, J. C. R. 1979 Highway modelling part 1: Prediction of velocity and turbulence fields in the wakes of vehicles. *Journal of Applied Meteorology* **18,** 387–400.

ESKRIDGE, R. E., BINKOWSKI, F. S., HUNT, J. C. R., CLARK, T. L. & DEMERJIAN, K. L. 1979 Highway modelling part 2: Advection and diffusion of SF6 tracer gas. *Journal of Applied Meteorology* **18,** 401–412.

ESKRIDGE, R. E. & RAO, S. T. 1983 Measurement and prediction of traffic induced turbulence and velocity field near roadways. *Journal of Applied Meteorology* **22,** 1431–1443.

ESKRIDGE, R. E. & RAO, S. T. 1986 Turbulent diffusion behind vehicles — experimentally determined mixing parameters. *Atmospheric Environment* **20,** 851–860.

ESKRIDGE, R. E. & THOMPSON, R. S. 1982 Experimental and theoretical study of the wake of block-shaped vehicles in a shear free boundary flow. *Atmospheric Environment* **16,** 2821–2836.

HARGREAVES, D. M. & BAKER, C. J. 1997 Gaussian puff model of an urban street canyon. *Journal of Wind Engineering and Industrial Aerodynamics* **69–71,** 927–939.

HIDER, Z. 1998 Modelling solute and particulate dispersion from road vehicles. Ph.D. thesis, University of Nottingham, U.K.

HOTCHKISS, R. S., & HARLOW, F. H. 1973 Air pollution transport in street canyons. Technical Report EPA R4 73 029, NTIS PB 233 252, prepared by Los Alamos National Laboratory for US Environmental Protection Agency.

HUCHO, W-F. 2000 Vehicle aerodynamics — present status and future development. *Proceedings of the MIRA Conference on Vehicle Aerodynamics*, Rugby, U.K.

IHT 1999 Air quality. Network management Note, Institution of Highways and Transport, London, U.K.

KASTNER-KLEIN, P., FEDOROVICH, E. & ROTACH, M. W. 1999 Organised and turbulent air motions in a wind tunnel model of a street canyon with and without moving vehicles. *Proceedings of 6th International Conference on Harmonisation within Atmospheric Dispersion Modelling*, Rouen, France

LOUKA, P., BELCHER, S. E. & HARRISON, R. G. 1998 Modified street canyon flow. *Journal of Wind Engineering and Industrial Aerodynamics* **74–76,** 485–493.

LOUKA, P., BELCHER, S. E. & HARRISON, R. G. 2000 Coupling between airflow in streets and the well developed boundary layer aloft. *Atmospheric Environment* **34,** 2613–2621.

MAIR, W. & STEWART, A. 1985 The flow past yawed slender bodies with and without ground effects. *Journal of Wind Engineering and Industrial Aerodynamics* **18**, 301–328.

MATSCHKE, G. & HEINE, C. 2000 Numerical computation of the wake of a six coach train set. *Proceedings of the CWE2000 Conference*, Birmingham, U.K., pp. 251–255.

MAULL, D. J. 1978 Mechanisms of two and three dimensional base drag. In *Aerodynamic Drag Mechanisms of Bluff Bodies and Road Vehicles* (eds G. Sovran, T. Morel & W. T. Mason Jr.) New York: Plenum Press, pp. 137–159.

NAMDEO, A. K., COLLS, J. J. & BAKER, C. J. 1999 Dispersion and resuspension of fine and coarse particulates in an urban street canyon. *Science of the Total Environment* **235,** 3–13.

NALPANIS, P., HUNT, J. C. R. & BARRETT, C. F. 1993 Saltating particle over a flat bed. *Journal of Fluid Mechanics* **251,** 661–685.

NAQA 2000 National Air Quality Archive web site, www.aeat.co.uk/netcen/airqual/welcome.html.

NOUZAWA, T., HIASA, K., NAKAMURA, T., KAWAMOTO, A. & SAT, H. 1992 Unsteady wake analysis of the aerodynamic drag of a notchback model with critical afterbody geometry, SAE paper 920202.

OKE, T. R. 1987 *Boundary Layer Climates*. New York and London: Routledge.

PEARCE, W. & BAKER, C. J. 1997 Wind tunnel investigation of the effect of vehicle motion on dispersion in urban canyons. *Journal of Wind Engineering and Industrial Aerodynamics* **69–71,** 915–926.

PEARCE, W. & BAKER, C. J. 1999 Wind tunnel tests on the dispersion of vehicular pollutants in an urban area. *Journal of Wind Engineering and Industrial Aerodynamics* **80,** 3, 327–349.

QUINN, A. D., BAKER, C. J. & WRIGHT, N. G. 2001 Wind and vehicle induced forces on flat plates; Part 2: Vehicle induced forces. *Journal of Wind Engineering and Industrial Aerodynamics* (in press).

RAO, S. T. & KEENAN, M. 1980 Suggestions for the improvement of the EPA-HIWAY model. *Journal of the Air Pollution Control Association* **30,** 247–256.

RAO, S. T. & SEFEDIAN, L. 1979 Characteristics of turbulence and dispersion of pollutants near major highways. *Journal of Applied Meteorology* **18**, 3, 283–293.

RICHARDS, K. A., WRIGHT, N. G., BAKER, C. J. & BAXENDALE, A. 2000a Computational modelling of pollution dispersion in the near wake of vehicles. *Proceedings of CWE2000 Conference*, Birmingham, U.K., pp. 77–80.

RICHARDS, K. A., WRIGHT, N. G., BAKER, C. J. & BAXENDALE, A. 2000b Computational modelling of pollution dispersion in the near wake of a vehicle. *Proceedings of MIRA Conference on Vehicle Aerodynamics*, Rugby, U.K.

ROBINSON, C. G. & BAKER, C. J. 1990 The effect of atmospheric turbulence on trains. *Journal of Wind Engineering and Industrial Aerodynamics* **34,** 251–272.

SEFEDIAN, L. & RAO, S. T. 1981 Effects of traffic generated turbulence on near field dispersion. *Atmospheric Environment* **15,** 527–536.

SIMS-WILLIAMS, D. B., DOMINY, R. G. & HOWELL, J. P. 2001 An investigation into large scale unsteady structures in the wake of real and idealized hatchback car models. SAE Paper — in press.

THOMSON, R. S. & ESKRIDGE, R. E. 1987 Turbulent diffusion behind vehicles; experimentally determined influence of vortex pair in vehicle wake. *Atmospheric Environment* **21,** 2091–2087.

TORRENCE, C. & COMPO, G. P. 1998 A practical guide to wavelet analysis. *Bulletin of the American Meteorological Society* **79,** 61–78.

YAMARTINO, R. J. & WIEGAND, G. 1986 Development and evaluation of simple models for the flow, turbulence and pollutant concentration fields within an urban street canyon. *Atmospheric Environment* **20,** 2137–2156.